A critical analysis of the X-ray photoelectron spectra of Ti3C2Tz MXenes

Varun Natu, Mohamed Benchakar, Christine Canaff, Aurélien Habrioux, Stéphane Célérier, Michel W Barsoum

A Critical Analysis of the X-Ray Photoelectron Spectra of $Ti_3C_2T_z$ MXenes

Varun Natu[‡], Mohamed Benchakar[Ⅱ], Christine Canaff[Ⅱ], Aurélien Habrioux[Ⅱ], Stéphane Célérier [Ⅱ], and Michel W. Barsoum[‡,]*

[‡] Department of Materials Engineering, Drexel University, Philadelphia, PA, USA

[Ⅱ] Institut de Chimie des Milieux et Matériaux de Poitiers (IC2MP), Université de Poitiers, CNRS, F-86073 Poitiers, France

*Corresponding author: barsoumw@drexel.edu

Abstract:

Since their discovery in 2011, the 2D transition metal carbide, nitrides, and carbonitrides - dubbed MXenes - have garnered a lot of worldwide interest. Given their 2D structure, surface, or termination, chemistries play a vital role in most applications. X-ray photoelectron spectroscopy, XPS, is one of the most common characterization tools for quantifying surface terminations and overall chemistry. Herein we critically review the XPS fitting models proposed for $Ti_3C_2T_z$ MXene in the literature and make the case that they are at best incomplete and at worst contradictory. We propose a new fitting algorithm based on all the data obtained from previously published studies. In our approach, we assign the Ti 2p peak at 455.0 eV, to the C-Ti-O\O\O and C-Ti-C octahedra. The peaks at 456.0, 457.0, 457.9, and 459.6 eV are assigned to C-Ti-O\O\F, C-Ti-O\F\F, C-Ti-F\F\F, and $TiO_{2-x}F_{2x}$, respectively. The first four represent possible Ti atom terminations; the last is an oxyfluoride. In our proposed model we do not distinguish between O and OH terminations in the Ti 2p spectra; we only do so in the O spectra. Lastly, we propose and recommend a method for quantifying the surface terminations in $Ti_3C_2T_z$.

Introduction:

After the discovery of 2D titanium carbide ($Ti_3C_2T_z$) - the first MXene - in 2011, nearly 30 new MXenes have been discovered so far in the last 10 years and several others are predicted to be stable according to computational calculations and are awaiting experimental realization.[1–3] MXenes show potential in various applications like energy storage and conversion,[4–6] photodetectors and sensors,[7] catalysts for various reactions,[8] reinforcement in polymer composites,[9] and electromagnetic interference (EMI) shielding,[10] among many others. MXenes are so labelled because they are obtained by selective etching of the A atomic layers from the parent MAX phases. The MAX phases have a general formula of $M_{n+1}AX_n$ where M stands for an early transition metal, X stands for C and/or N and A is mostly a group 13 or 14 element.[11–13] Because when the Al layers are etched they are replaced by surface terminations, the general formula of MXenes is $M_{n+1}X_nT_z$, where T_z represents surface terminations that are typically a combination of –O, –OH, and/or –F.[14] The -ene suffix was added to signify their similarity to other 2D materials like graphene.[1] Recently discovered MXene synthesis technique of using molten salt to etch out the A layer leads to terminations like -Cl, -Br, and -I, and further chemical modifications can also result in -S, -Te, and -NH terminations.[15,16]

Given the 2D morphology of MXenes, their surface chemistries play an important role in determining their properties. For example, surface terminations are responsible for the spontaneous ion intercalation and exchange in between MXene layers.[17] They are also responsible for the hydrophilicity of MXenes which makes it one of the most easily processable 2D material.[18] In energy storage devices like supercapacitor and batteries, MXene surface terminations are shown to participate in the charge storage mechanism.[19] Recent work by

Kamysbayev *et al*. showed that superconductivity in Nb_2CT_z is dependent on the type of surface terminations.[16] The work function of MXenes can also be tuned by modifying its surface groups making them good electronic contacts in circuits.[20] Apart from these applications, MXene surface terminations have also been shown to play a role in influencing optical, mechanical, magnetic and, a multitude of other properties.[21]

Due to the critical role surface terminations play on properties, it is important to characterize them properly. There a number of techniques that can do so including, X-Ray photoelectron spectroscopy (XPS), X-ray adsorption spectroscopy (XAS),[22] nuclear magnetic resonance spectroscopy (NMR),[23,24] Raman spectroscopy,[25] and transmission electron microscopy (TEM) coupled with electron energy loss spectroscopy (EELS).[26,27] XPS remains the most widely used of all the techniques. There are several advantages of using XPS to analyze MXenes as it is sensitive to all the elements except H and He.[28] It can be used to analyze bonding environments of constituent elements, quantify the elemental compositions including terminations, and detect small concentrations of elements especially if they are at the surfaces.[28] Other advantages include non-destructive sample preparation and the fact that restrictions on sample size and form are low. XPS spectrometers are widely available in most university settings and large research and development laboratories.

To date, four studies have focused on understanding and fitting XPS spectra on $Ti_3C_2T_z$ flakes.[14,20,29,30] As discussed below, while there are similarities between the various fitting protocols, there are also some inconsistencies that can sow confusion. In this review, we summarize XPS fitting models proposed in the literature especially for $Ti_3C_2T_z$ and, propose a new fitting model, based on the critical analysis of previously published studies. In our model,

we fit the XPS spectra based on nature of the surface termination surrounding each Ti atom, rather than the oxidation states of Ti as many, including us, have previously done. We also argue that the ambiguity in the fitting is higher in the O and F spectra compared to the Ti and C high-resolution spectra.

Before going into a detailed discussion of the various fits, it should be noted that the Ti 2p spectrum has 2 peaks at roughly 455 and 463 eV corresponding to Ti $2p_{3/2}$ and Ti $2p_{1/2}$ respectively. The Ti 2p peak is split into 2 peaks due to spin-orbit splitting and both peaks contain information about the Ti bonding environment . Therefore, when component peak fitting is used to deconvolute these peaks, all components fit under the Ti $2p_{3/2}$ peak are also fit in the Ti $2p_{1/2}$ peak (further details are given later in the Titanium section). Component peaks are fit to understand what species of Ti are present and from here onwards in the discussion of the various regions whenever 'peaks' are mentioned we refer to the component peaks used to fit the spectra and not the envelope peaks.

Fit-I

The first detailed study dedicated to understand the XPS spectra of $Ti_3C_2T_z$ was carried out by Halim *et al.* in 2016.[14] They based their fittings on the oxidation states of Ti and attribute the first 3 peaks at 455.0 eV, 455.8 eV, and 457.2 eV to Ti^{+1}, Ti^{+2}, Ti^{+3} oxidation states, respectively (Fig. 1a, Table 1). The peak separation between the Ti $2p_{3/2}$ and $2p_{1/2}$, Δ_{Ti2p}, caused by spin-orbit splitting (see below) was kept fixed at 6.2 eV, 5.5 eV, and 5.7 eV for the Ti^{+1}, Ti^{+2}, Ti^{+3} peaks, respectively (Table 1).[14] This Δ_{Ti2p} is consistent with other XPS studies on Ti metal and related compounds such as titanium carbide, TiC where the peak separation is found to be ~ 6.1-6.2 eV.

The Δ_{Ti2p} in TiO (Ti^{+2}) is ~ 5.6-5.7 eV and that for Ti_2O_3 (Ti^{+3}) is ~ 5.7 eV. [31,32] In our proposed fit (see below) a Δ_{Ti2p} of 6.1 eV was used for all Ti peaks related to $Ti_3C_2T_z$.

The C-Ti-F component peak was set at 460.2 eV, with a Δ_{Ti2p} of 6 eV (Table 1). These values are consistent with fluorinated Ti compounds like TiF_3.[33] The last set of Ti peaks found around 459.3 eV (Δ_{Ti2p}= 5.6 eV) and 460.2 eV (Δ_{Ti2p}= 6 eV) (Fig. 1a, Table 1) were ascribed to TiO_2 and $TiO_{2-x}F_{2x}$ oxides, respectively, formed due to the degradation/oxidation of $Ti_3C_2T_z$ by reaction with ambient air and/or water. Note that Halim *et al*. assumed these two components not to originate from the $Ti_3C_2T_z$ flakes themselves, but rather from their oxides and oxyfluorides. We make the same assumption below.

Irrespective of the type of termination present, the C 1s high-resolution spectra associated with $Ti_3C_2T_z$ all appear in the quite narrow range of ≈ 281.9-282.0 eV (Fig. 1b, Table 1). This signal originates from C-atoms residing in the Ti octahedra. The rest of the components are typically ascribed to C contamination introduced during synthesis or from ambient air. This is so universal in $Ti_3C_2T_z$ synthesized in F-ion containing acids that it can be used as a check on the calibration of the XPS spectra. As discussed below, there are some exceptions (for details see **Carbon (C 1s)** section).

In the O 1s spectra (Fig. 1c, Table 1), two components associated with $Ti_3C_2T_z$ flakes were set at 531.2 eV and 532.0 eV and ascribed to -O and -OH terminations, respectively. Three other peaks were added to the fitting at 529.9 eV, 532.8 eV, and 533.8 eV corresponding to, respectively, TiO_2, Al_2O_3, and adsorbed or interlayer water (Table 1). Contributions from C-O, C=O, -COOH, etc. species from the adventitious C tend to overlap with the components described earlier

making their estimation difficult and probably leading to overestimation of some of the components in the O 1s spectra.

The F 1s spectra were fit with 4 components corresponding to C-Ti-F, $TiO_{2-x}F_{2x}$, $AlF_{x,}$ and $Al(OF)_x$ at 685.0, 685.3, 686.4, and 688.3 eV, respectively. With only 38 % of the total photoemission spectra attributed to the C-Ti-F of MXene itself, the majority was due to the aforementioned impurities.

Henceforth, this model proposed by Halim *et al.* will be referred to as Fit-I.

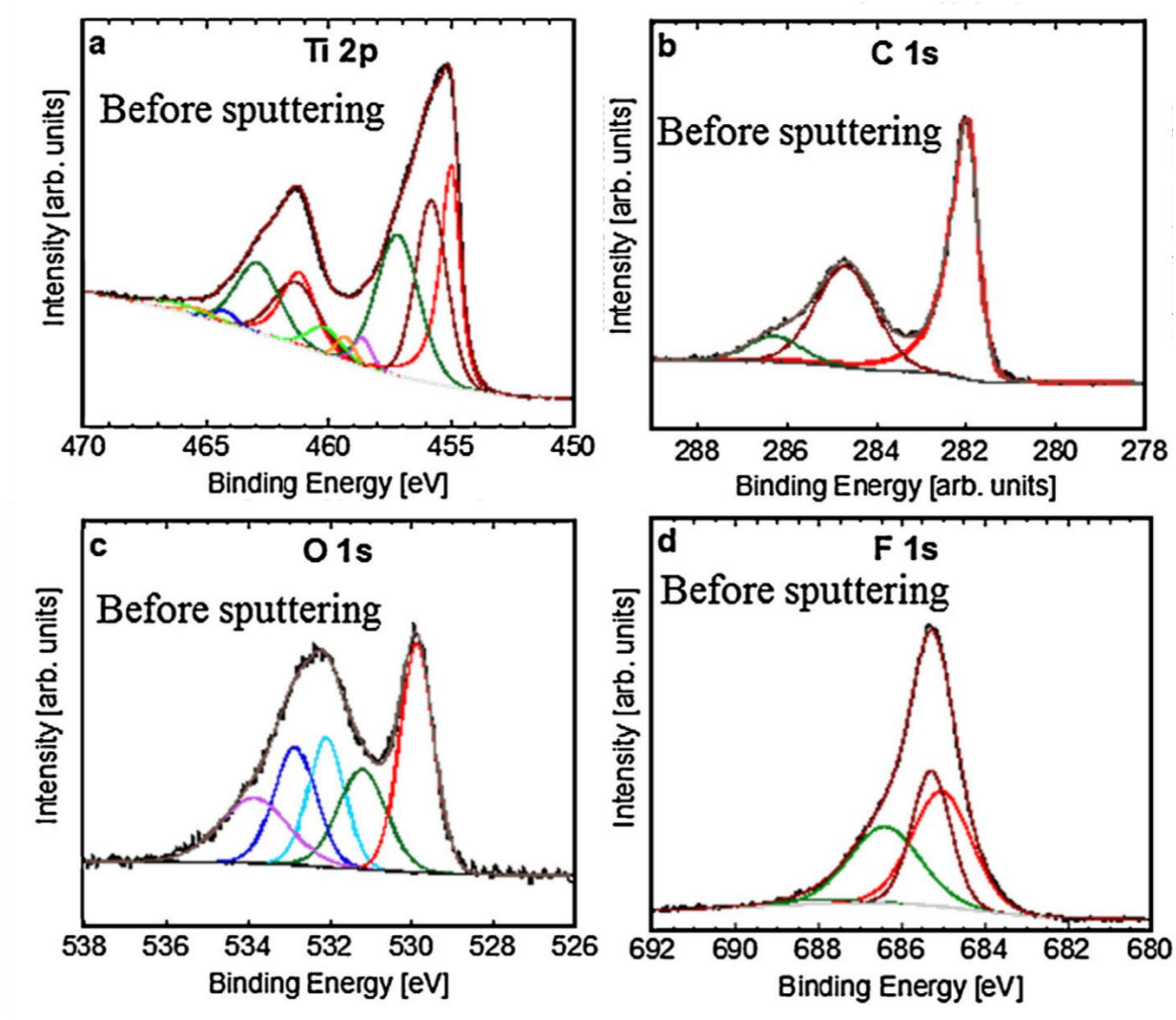

Figure 1: Component peak fits of XPS spectra of as-prepared $Ti_3C_2T_z$ powders. High-resolution component peak fits of, a) Ti 2p, b) C 1s, c) O 1s, and d) F 1s regions.[14]

Table 1: Summary of XPS peak fits by Halim *et al*. shown in Figure 1.[14] The $Ti_3C_2T_z$ sample was prepared by etching the MAX phase in 48% HF. Binding energies BE and full-width at half maximum, FWHM, values of the Ti $2p_{3/2}$ peaks are listed in columns 2 and 3, respectively. Respective numbers for Ti $2p_{1/2}$ peaks are shown in brackets.

Region	BE (eV)	FWHM (eV)	Fraction	Assigned to
Ti $2p_{3/2}$ ($2p_{1/2}$)	455.0 (461.2)	0.8 (1.5)	0.28	C-Ti-(O/OH)
	455.8 (461.3)	1.5 (2.2)	0.30	C-Ti^{2+}-(O/OH)
	457.2 (462.9)	2.1 (2.1)	0.32	C-Ti^{3+}-(O/OH)
	458.6 (464.2)	0.9 (1.0)	0.02	TiO_2
	459.3 (465.3)	0.9 (1.4)	0.03	$TiO_{2-x}F_{2x}$
	460.2 (466.2)	1.6 (2.7)	0.05	C-Ti-F
C 1s	282.0	0.6	0.54	C-Ti-(O/OH/F)
	284.7	1.6	0.38	C-C
	286.3	1.4	0.08	CH_x/C-O
O 1s	529.9	1.0	0.29	TiO_2
	531.2	1.4	0.18	C-Ti-O_x and/or OR
	532.0	1.1	0.18	C-Ti-OH_x and/or OR
	532.8	1.2	0.19	Al_2O_3 and/or OR
	533.8	2.0	0.17	H_2O and/or OR
F 1s	685.0	1.7	0.38	C-Ti-F
	685.3	1.1	0.29	$TiO_{2-x}F_{2x}$
	686.4	2.0	0.30	AlF_x
	688.3	2.0	0.02	$Al(OF)_x$

Fit-II:

Persson *et al*.[29] proposed a different fitting model. They based their fits on the crystal sites that the various atoms occupy.[29] When dealing with the Ti spectra, they differentiated between C-Ti-O\O\O, C-Ti-(O, F), and C-Ti-F\F\F. In this notation, used henceforth, the atoms separated by

"\" are the terminations present. For example, C-Ti-O\O\O corresponds to Ti atoms in octahedra with 3 C atoms and 3 O surface atoms at the vertices. In C-Ti-F\F\F, all the terminations are F. The notation C-Ti-(O,F) represents mixed O and F-terminations.[29]

Their fits are based on density functional theory (DFT) calculations by Khazaei *et al.* who found two thermodynamically favorable sites on MXene surfaces: A sites A corresponding to surface group occupying positions above the central Ti atom (so-called FCC sites) and B sites corresponding to surface group above the C atoms right below the surface Ti atoms (Figs. 2d,e).[34]

The Ti $2p_{3/2}$ peak was fit with 3 components corresponding to C-Ti-O\O\O, C-Ti-(O,F), and C-Ti-F\F\F at 455.1 eV, 455.9 eV, and 456.9 eV, respectively (Fig. 2c, Table 2). As just noted, because Persson *et al.* do not distinguish between the C-Ti-O\O\F, C-Ti-O\F\F configurations; they only assigned one peak for the two at 455.9 eV. The Δ_{Ti2p} was kept constant for all components and fixed at 6.1 eV. Also, no oxide peaks were included in the fits as the authors scanned MXenes right after etching and washing with minimal exposure to ambient air.

The O 1s spectra were fit with 3 peaks, 2 of which were assigned to -O terminations occupying the A and bridging sites, while the third was assigned to a -O co-absorbed with -F on the A sites. The respective energies were 531.3, 529.9, and 531.9 eV (Fig. 2b, Table 2). Similarly, in the F 1s spectra, 2 peaks were observed at 684.5 eV and 685.4 eV corresponding to -F terminations and -F terminations co-adsorbed with O (Fig. 2a, Table 2). Similar to Fit-I, only one C 1s peak at 282.0 eV was ascribed to the MXene flakes; the rest were ascribed to adventitious C contaminations.

This fitting model proposed by Persson *et al*., will henceforth be referred to as Fit-II.

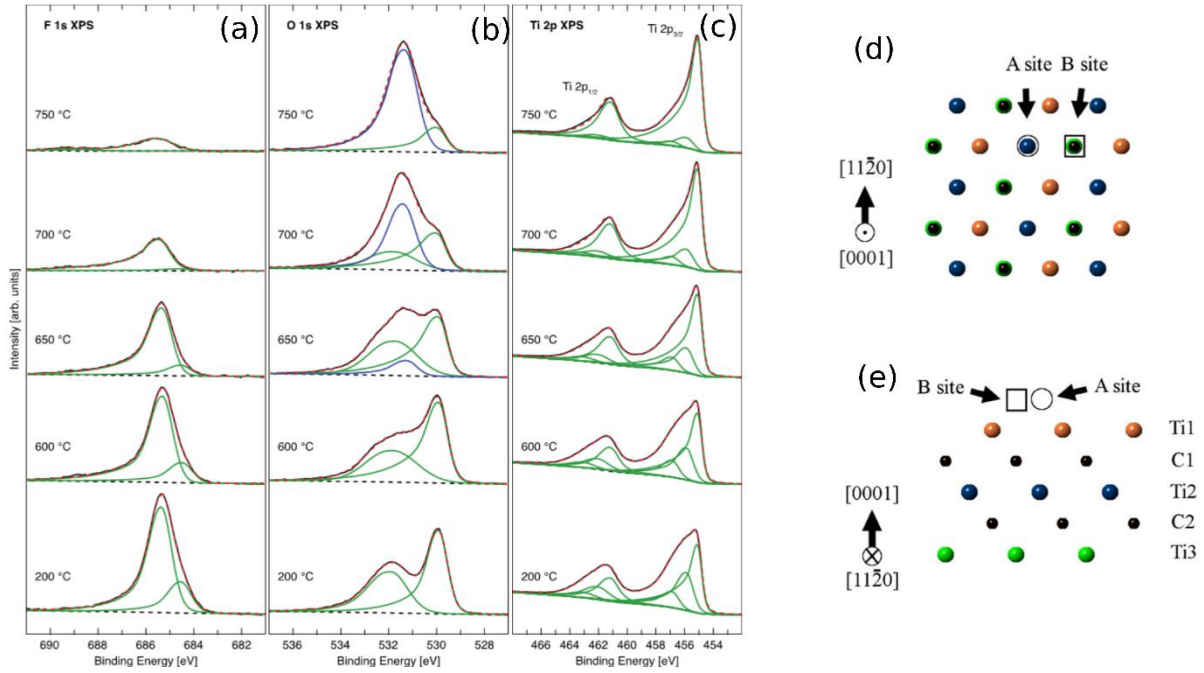

Figure 2: Peak fits of XPS spectra of $Ti_3C_2T_z$ MXene during in-situ vacuum annealing inside a XPS chamber at various temperatures. High-resolution component peak fits of, a) F 1s b) O 1s, c) Ti 2p, and d) F1s regions ; d) top and e) side view with A and B possible termination sites.[29]

Table 2: Summary of XPS peak fits shown in Figure 2. The $Ti_3C_2T_z$ sample was prepared by etching the MAX phase in 10 % HF. Binding energies BE and FWHM values of Ti $2p_{3/2}$ peaks are listed in columns 2 and 3, respectively. Respective numbers for the Ti $2p_{1/2}$ peaks are shown in brackets.[29] This summary is only of the fits after annealing at 200 °C.

Region	BE (eV)	FWHM (eV)	Assigned to
Ti $2p_{3/2}$ ($2p_{1/2}$)	455.1 (461.2) 455.9 (462.0) 456.9 (463.0)	0.7 (1.4) 1.1 (1.9) 1.1 (1.9)	C-Ti-O\O\O C-Ti-(O, F) C-Ti-F\F\F
C 1s	282.0 284.3 285.2 286.4	0.64 1.3 1.3 1.3	Ti-C-Ti C-C CH_x C-OH
O 1s	529.9 531.3 531.9	0.89 1.2 1.6-2.3	C-Ti-O (bridging) C-Ti-O (A-site) C-Ti-O/F (A-site)
F 1s	684.5 685.4	1.0 1.0	C-Ti-F C-Ti-O, F

Fit-III:

Similar to Persson *et al*.[29], Schultz *et al*. also measured XPS *in situ* as a function of heating but they used a different fitting model (Fig. 3, Table 3).[20] Three components were fit in the Ti $2p_{3/2}$ spectra (Fig. 3g) corresponding to C-Ti-C, C-Ti-O, and C-Ti-F at 455.2 (Δ_{Ti2p}=5.9 eV), 456.2 (Δ_{Ti2p}=5.4 eV) and 457.3, eV (Δ_{Ti2p}=5.4 eV), respectively (Fig. 3g, Table 3). The first peak was assigned to Ti bonded to C only – i.e. the central Ti atoms labelled Ti2 in Fig. 3b - while the second and third peaks were assigned to Ti atoms bonded to pure O- and pure F-terminations, respectively (Fig. 3g). In this model, the assumption was made that the central Ti atoms surrounded octahedrally with 6 C atoms can be differentiated from the ones closer to the surfaces. As discussed below, such differentiation is not trivial to say the least.

In the O 1s spectra, 3 related components were fit at 529.8, 531.6, and 533.8 eV corresponding to bridging O-terminations (Fig. 3h), O-terminations at A/B sites (Figs. 3b,c), and OH terminations at A/B sites. Schultz et al. claimed that the OH component overlaps with adsorbed water making those two difficult to distinguish. Only one component for the C and F spectra corresponding to MXene was fit at 291.9 eV and 685.2 eV, respectively, the remainder were ascribed to impurities (Fig. 3f, i, Table 3). Henceforth this fit proposed by Schultz *et al*. will be referred to as Fit-III. The differences between this fit and the previous two should be clear at this point.

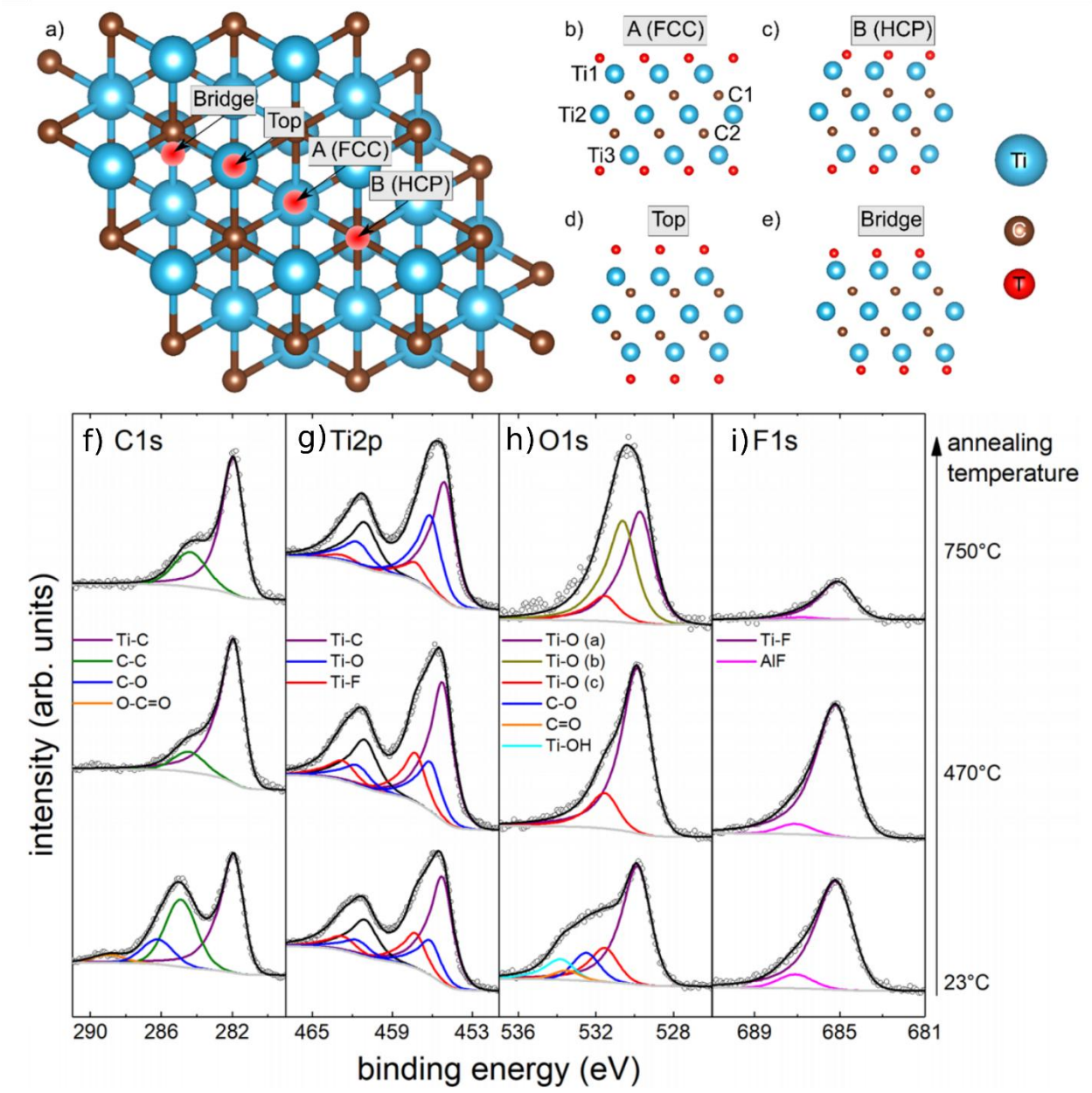

Figure 3: a) Top and b-e) side views with possible termination sites. Peak fits of XPS spectra of $Ti_3C_2T_z$ during *in situ* vacuum annealing inside an XPS chamber at various temperatures. High-resolution component peak fittings of, f) C 1s, g) Ti 2p, h) O 1s, and i) F1s region.[20]

Table 3: Summary of XPS peak fits shown in Figure 3. Sample was prepared by etching Ti_3AlC_2 in a LiF+HCl mixture. Numbers in brackets in column 2 are peak locations for Ti $2p_{1/2}$ while the BE values the Ti $2p_{3/2}$ peaks are listed outside the brackets.[20] These values correspond to fits of spectra collected at RT.

Region	BE (eV)	Assigned to
Ti $2p_{3/2}$ ($2p_{1/2}$)	455.2 (461.1)	Ti-C
	456.2 (461.6)	Ti-O
	457.3 (462.7)	Ti-F
C 1s	281.9	Ti-C-Ti
	284.9	C-C
	286.2	C-O
	288.9	C=O
O 1s	529.8	C-Ti-O (Bridge)
	531.6	C-Ti-O (A/B site)
	532.5	C-O
	533.4	C=O
	533.8	Adsorbed H_2O or C-Ti-OH
F 1s	685.2	C-Ti-F
	687.1	F-contamination

Fit-IV:

In a recent paper, Benchakar *et al*.[30] used as similar approach to that of Halim *et al*. in the Ti 2p region, except the component at ~ 460.0 eV, which was ascribed to -F terminations by Halim *et al*., [14] was ascribed to a titanium fluoride (TiF_x) salt formed due to over-etching (Fig. 4, Table 4).[30]

The O 1s fits, on the other hand, used aspects of the fits I and III. The -O terminations at A and the bridging sites were similar to those of Fit-III (Table 1,3,4), respectively assigned to C-Ti-O(ii) and C-Ti-O(i) in Table 4 and Figure 4. An -OH component similar to Fit-I was also assumed. Peaks for organic contamination and titanium oxyfluoride ($TiO_{2-x}F_{2x}$) were also added. Note that the contribution of titanium oxide and oxyfluoride in the O1s region at 530.6 and 529.9 eV, respectively are not at the same as those of Halim *et al.* Similar to previous studies, only one

component in the F 1s and C 1s regions was fit (Fig. 4, Table 4). Henceforth this model will be referred to as Fit-IV.

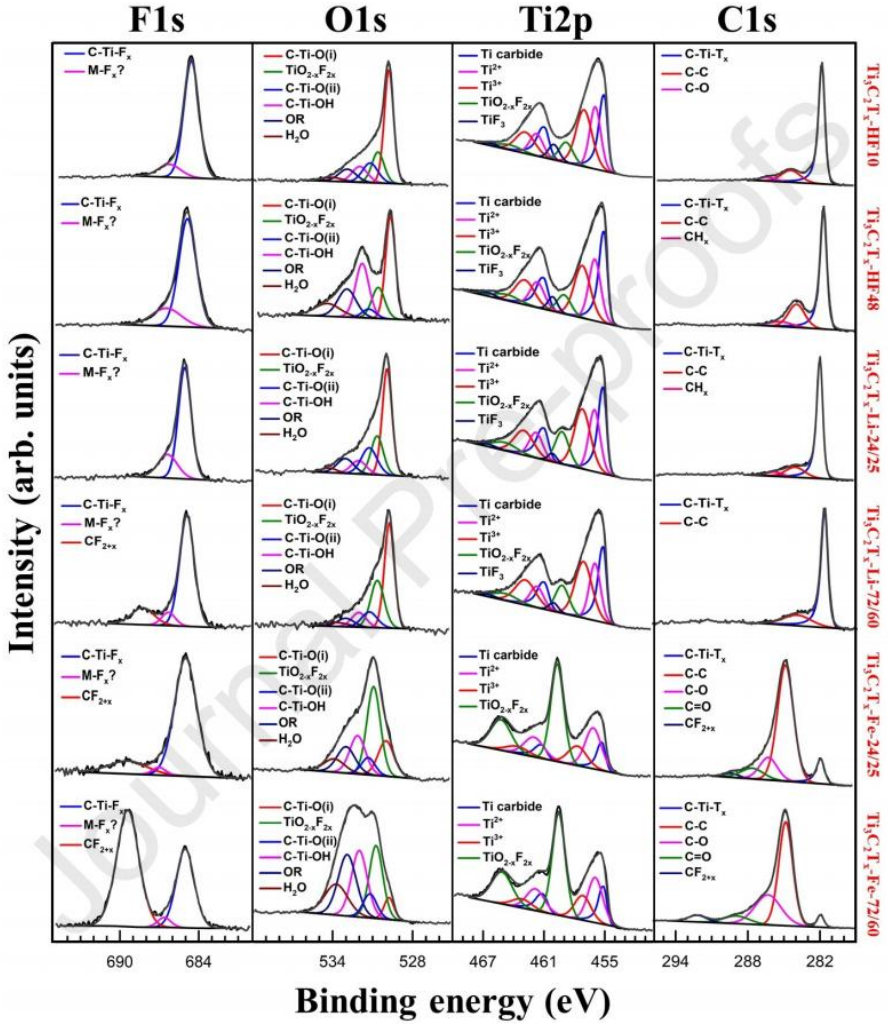

Figure 4: Peak fits of XPS spectra (according to Benchakar *et al.*) of $Ti_3C_2T_z$ synthesized using different conditions indicated on right-hand side.[30] In Table 4, we only list the results of the topmost panels, viz. MXene etched using 10 % HF.

Table 4: Summary of XPS peak fits for MXene synthesized using 10% HF shown in top of Figure 4. Binding energies BE and FWHM values of the Ti $2p_{3/2}$ peaks are listed in columns 2 and 3, respectively. Respective numbers for Ti $2p_{1/2}$ peaks are shown in brackets.[30]

Region	BE (eV)	FWHM (eV)	Fraction	Assigned to
Ti $2p_{3/2}$ ($2p_{1/2}$)	455.0(461.0)	0.8 (1.1)	9.95	C-Ti^{+1}-(O/OH/F)
	455.8 (461.7)	1.3 (1.6)	10.16	C-Ti^{2+}-(O/OH/F)
	457.0 (462.8)	1.9 (2.3)	12.54	C-Ti^{3+}-(O/OH/F)
	458.9 (464.6)	1.6 (2.9)	3.76	$TiO_{2-x}F_{2x}/TiO_2$
	460.0 (466.4)	1.2 (1.8)	1.87	TiF_x
C 1s	281.9	0.6	22.65	C-Ti-(O/OH/F)
	284.4	1.8	5.22	C-C
	286.4	1.9	0.74	C-O
O 1s	529.7	0.8	8.86	C-Ti-O(i)
	530.6	1.2	3.15	$TiO_{2-x}F_{2x}$
	531.2	1.4	2.55	C-Ti-O(ii)
	532.0	1.4	2.04	C-Ti-OH
	533.0	1.5	1.85	OR
	533.7	2.2	0.69	H_2O
F 1s	685.0	1.3	12.30	C-Ti-F
	686.6	1.6	1.65	F-contamination

Critical Analysis

Based on these 4 important studies, it is clear that there is no clear consensus in the MXene community about the interpretation of $Ti_3C_2T_z$ XPS spectra. In Fits-I, II, and IV the first peak in the Ti $2p_{3/2}$ spectra is at ~ 455.0 eV is assigned to C-Ti-T_z, while in Fit-III it is assigned to Ti-C-Ti. The discrepancies in BEs of the C-Ti-F components are even larger than those of C-Ti-O. In Fits I and II there is a 3.3 eV difference in the BEs of the respective C-Ti-F peaks. In Fits-I and III that difference is 2.9 eV. Fit-IV does not account for a separate C-Ti-F peak since it is claimed that these peaks overlap with those of the C-Ti-O/OH peaks and thus cannot be distinguished. Apart from these two peaks, other peaks in Fits-I, II and III are assigned to different species making a direct comparison between the BEs impossible. Needless to add these

are serious problem. What renders the problem even more confusing is that most other studies that use XPS for characterization of $Ti_3C_2T_z$, use either of these 4 models or, even in some cases, a mix of them. The purpose of this paper is to critically assess these four fits and recommend a less confusing way forward.

Generally, due to some samples charging during XPS measurements, the spectra obtained tend to shift to higher BE values. To counter this issue, the spectra need to be calibrated. Here there are a number of approaches. One sets the BE of C-C bonds from adventitious carbon to ~284.8 eV. One problem with this method is that it relies on C impurities whose BE values is not well agreed upon and several reports have used values anywhere between 284.5-285.0 eV making reliable calibration difficult.[35] This 0.5 eV difference does not allow for accurate calibration.[35] The second method is to add powders of noble metals like Au or Ag to the samples, with well-known BEs.[36] This method has never been used in the MXene literature and is not discussed further.

The third, and highly recommended herein, is aligning the Fermi edge of the spectra to 0 eV. This is an efficient and accurate method of calibration.[35] Therefore the C-C B.E should be used for calibration only be when Fermi edge is not sharp or the C-Ti-C peak in the C 1s spectra of $Ti_3C_2T_z$ is not at 282.0 eV (Details of C 1s spectra fitting are discussed later). In the 4 fits discussed above, Halim *et al.*[14] (Fit-I) and Persson *et al.*[29] (Fit-II) uses the Fermi edge for calibration, while Benchakar *et al.*[30] (Fit-IV) set the Ti-C-Ti peak BE in the C 1s spectra to 281.9 eV. Schultz *et al.*[20] (Fit-III) do not mention their method of calibration.

In the following, we discuss each element separately.

Carbon (C 1s):

As shown in Table 5, the C 1s BE values are quite reproducible between studies. That peak lies at 282.0±0.06 eV. This also implies that the BE of the C atoms in the octahedral sites, viz. Ti-C-Ti, are *not affected* by the type of surface terminations attached during etching in F-ion containing acids. It also seems to be independent of the M:X ratio, viz. n in $Ti_{n+1}X_nT_x$, or the presence of nitrogen, N, in neighboring X sites.

Over the 7 studies listed in Table 5, the standard deviation in the BE values is only 0.06 eV. It follows that this BE is an important anchor point that if not found suggests problems with the XPS spectra, most likely with calibration and/or the absence of MXenes. Therefore, in cases where the Fermi edge is not sharp enough to use for calibration, we recommend setting the BE in the C 1s spectra to 282.0 eV. It should be noted that this calibration works well with MXenes synthesized in F-containing acids. In recently discovered molten salt synthesized MXenes, initial XPS studies suggest the Ti-C-Ti peaks deviate from 282.0 eV (see below).

The BE of a purely covalent C=C bond is ≈ 284.5 eV[37]. The Ti-C-Ti BE of 282.0 eV in $Ti_{n+1}C_nT_z$, implies the C atoms are withdrawing electrons from the Ti atoms, which is fairly well established for MXenes at this point.[22] The relationship between the M-C-M component BE and Pauling's electronegativity, EN, of the M in the MXene is plotted in Figure 5 and listed in Table 6. These results indicate that the bond polarity decreases as the EN difference between M and C atoms goes down and that the 282.0 eV value is thus only valid for $Ti_3C_2T_z$ and even then, as discussed below, only under certain circumstances.

Table 5: C 1s BE values of C-Ti-T_z peaks from literature. Note values were taken only from studies where the Fermi edge was used for calibration of the XPS spectra.

MXene	Etching method	BE (eV)	FWHM (eV)	Reference
$Ti_3C_2T_z$	50 % HF	282.0	0.6	[14]
	LiF + HCl	282.0	0.6	[17]

	NH_4HF_2 10 % HF etched NaOH treated Vacuum annealed up to 700 °C	281.9 282.0 282.0	0.6 0.6 0.6	[38] [39] [29]
Ti_2CT_z	10 % HF	281.9	0.6	[14]
Ti_3CN	30 % HF	282.1	0.7	[14]
	Average	282±0.06		

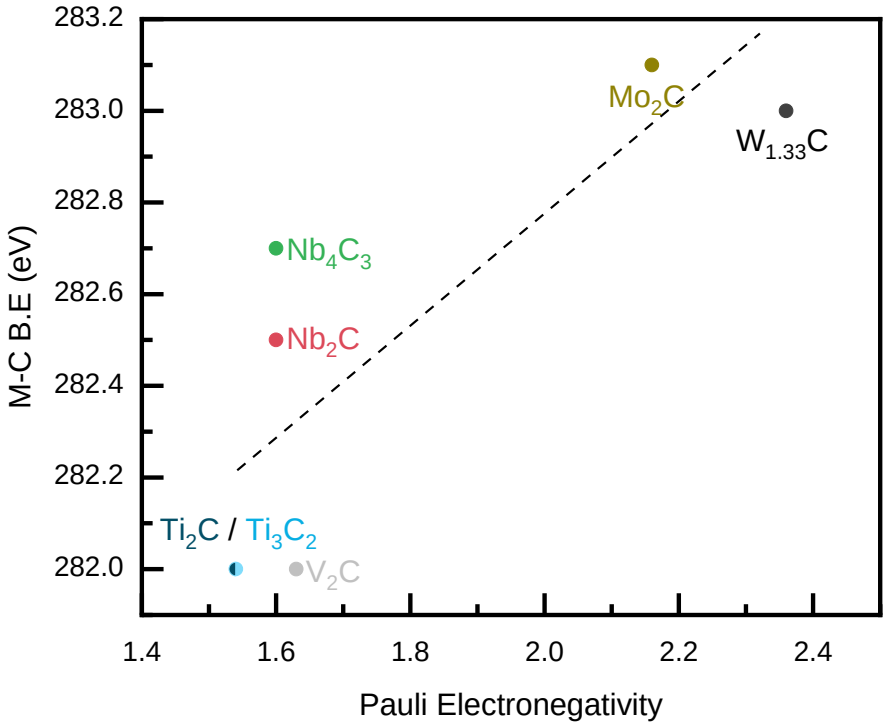

Figure 5: BE of C-M-T_z component in C 1s spectra plotted vs EN of transition metal. Values were taken only from studies where the Fermi edge was used for calibration of XPS spectra.[14,40–42] Dotted line is a guide to the eyes.

Table 6: BE values of C-M-Tz components of various MXenes as plotted in Figure 5.

MXene composition	BE of C-M-T_z (eV)	Reference
Ti_2CT_z	281.9	11
V_2CT_z	282.0	37
Nb_2CT_z	282.5	11
$Nb_4C_3T_z$	282.7	11

Mo_2CT_z	283.1	35
$W_{1.33}CT_z$	283.0	36

Titanium (Ti 2p):

Before discussing the details of fitting the Ti 2p spectra, several important considerations need to be established. More specifically,

1) The Ti 2p spectra are always split into 2 main peaks corresponding to Ti $2p_{3/2}$ and Ti $2p_{1/2}$. Any component fit to a Ti $2p_{3/2}$ peak should also be used to fit the Ti $2p_{1/2}$ peak. In theory, the area ratio between the two should be exactly 2:1, but in practice, due to imperfect background subtraction, possible overlapping of satellite peaks and the Coster-Kronig effect the area ratios may slightly deviate from expected.[43]

2) The separation Δ_{Ti2p} between the Ti $2p_{1/2}$ and Ti $2p_{3/2}$ peaks should be consistent for all components assigned to the same material. Here Δ_{Ti2p} for $Ti_3C_2T_z$ related peaks is set to 6. 1eV and for oxides and oxyfluorides it is set to 5.7 eV.

3) Because MXenes are highly conductive, the component peaks should have asymmetric line shapes instead of the commonly used symmetric Gaussian line shapes. As shown in Figures 6a,b, the same Mo 3d spectra of a Mo_2CT_z MXene are fit using both asymmetric (Fig. 6a) and symmetric peaks (Fig. 6b). In the latter, an extra, unphysical, Mo component is needed to achieve a good fit. This component is not needed when the correct asymmetric peaks are used. Here Mo_2CT_z was chosen as an example to make this point because only one component is fitted in the Mo 3d spectra which reduces the ambiguity about the number of peaks.

4) Instead of the more commonly used Shirley background, for $Ti_3C_2T_z$ we suggest to use a Tougaard background instead as it has been shown to give better quantitative results especially for transition metal-based compounds.[28,44] For consistency, a Tougaard background was used for the C 1s, O 1s, and F 1s spectra as well. Some MXene studies have assumed a linear background. This should be avoided as the linear background does not have a physical underpinning like the Shirley or Tougaard backgrounds.[28,44] That being said, more detailed analysis is necessary to understand which background works the best for MXenes as even under Tougaard or Shirley background several different variations like iterated Shirley, 2 or 3 parameter Tougaard, etc. are possible."

5) Due to several components being fit in a broad envelop currently it is not possible to resolve the FWHM of each component independently. Therefore, we propose to set the FWHM of MXene related components fits under the Ti $2p_{3/2}$ to be equal. The same for the Ti $2p_{1/2}$; we constrained them have equal FWHM. Note that does not imply that the FWHM are the same for both; In general, the Ti $2p_{1/2}$ components have broader FWHM compared to their Ti 2p3/2 counterparts due to the Coster-Kronig effect.

Though the above 5 points might seem basic to the XPS community, they are at times ignored in the MXene literature which can lead to false interpretations.

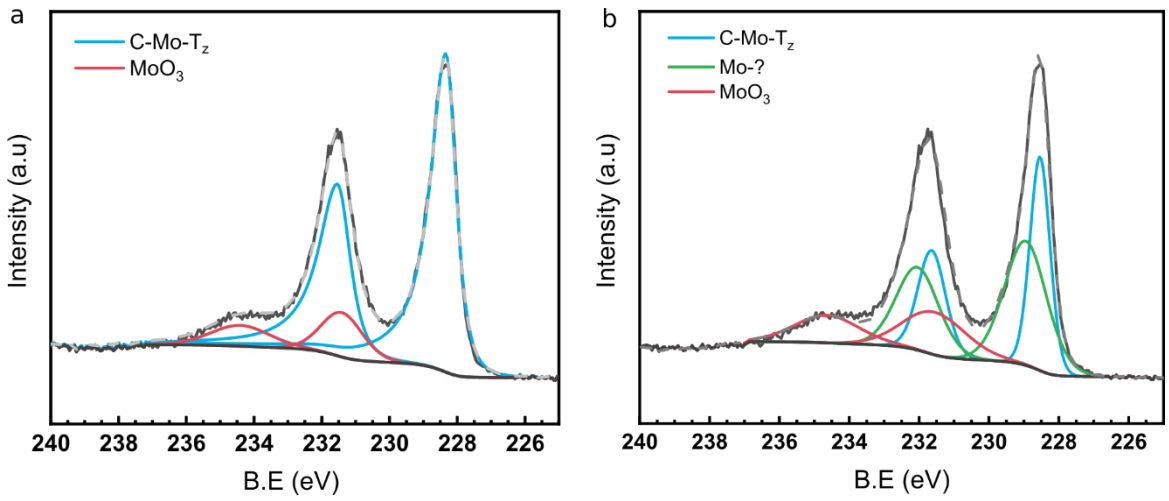

Figure 6: Peak fitting of Mo 3d spectra Mo_2CT_z MXene using, a) asymmetric peaks and b) symmetric peaks for the C-Mo-T_z component. Raw data were obtained from Ref [5] and refit for this figure.

$Ti_3C_2T_z$ vs. Ti_2CT_z

In Fit-III, Schultz *et al*. differentiate Ti bonded to 6 C atoms and those bonded to only 3. They assigned the former with a BE of 455.2 eV. Figures 7a, b depict the crystal structures of Ti_2CT_z and $Ti_3C_2T_z$, respectively. The Ti atoms circled in blue, shown in both figures, have identical bonding environments; they are bonded to 3 C atoms and 3 T-atoms (Fig. 7c). The Ti atoms in the middle layer of the Ti_3C_2 slab, circled in brown, are surrounded by 6 C atoms. Said otherwise these Ti atoms sit in the centers of C-octahedra (Fig. 7d). So, in principle, there should be 2 distinct components, with the C-Ti-C atoms having a lower BE than the C-Ti-T site since the EN of C is lower than that of O, F, Cl, etc., and should match closely that of Ti in cubic TiC (454.6 eV[45]). More importantly, the C-Ti-C atoms should be absent from the Ti 2p spectra of Ti_2CT_z. However, when we overlay typical Ti 2p spectra of both MXenes (Fig. 7e) it is evident that at lower BEs – to the right of the dashed line - the overlap is excellent. It follows that the C-Ti-C site in $Ti_3C_2T_z$ is indistinguishable from the C-Ti-T_z site by conventional XPS and therefore the

assignment of the 455.2 eV peak to the C-Ti-C site in Fit-III and other studies,[46–48] is wrong. As discussed below this result may be because the charge on the C atoms in $Ti_3C_2T_z$ is ≈ -2. The deviations between the two Ti spectra at higher BEs are probably due to the difference in the associated -F termination. This comment notwithstanding, more detailed studies using high-resolution synchrotron facilities in tandem with DFT are needed to better understand why the two Ti sites are apparently indistinguishable.

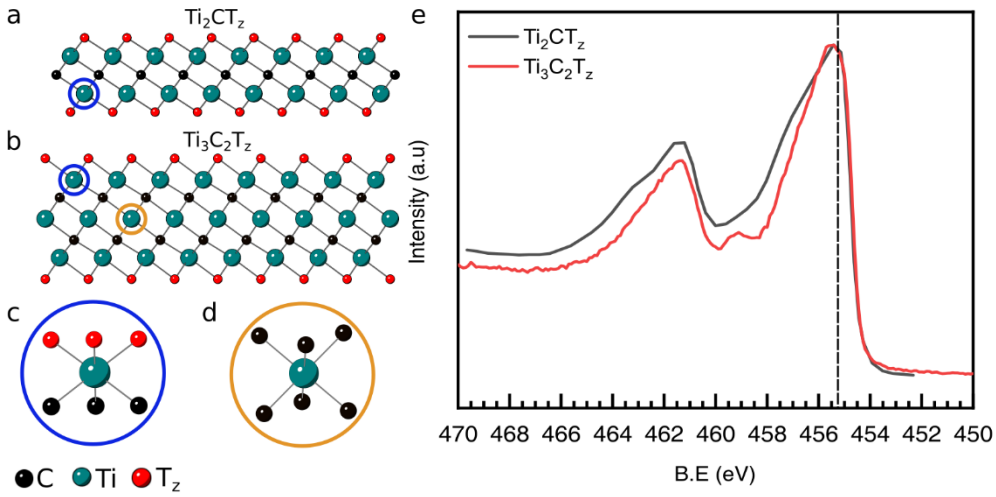

Figure 7: a) Crystal structures of Ti_2CT_z and b) $Ti_3C_2T_z$ MXenes; c) and d) magnified views of Ti atoms circled blue and brown in a and b with different bonding environment; e) Ti 2p spectra of Ti_2CT_z (grey) and $Ti_3C_2T_z$ MXene.

Do the Ti MXene peaks correspond to Ti oxidation states or local environments?

If care is not taken during etching and, more importantly, the storage of $Ti_3C_2T_z$ flakes, they will oxidize, usually to rutile and/or anatase TiO_2.[49,50] If that is the case, it is crucial to be able to differentiate the Ti atoms terminated by O atoms and those in separate oxide or oxyfluoride particles. This problem is quite acute if during etching the C atoms are replaced by O atoms as shown by Yoon *et al*.[51] In this review, we assume that the Ti and C lattice site ratio is preserved

at 3:2, respectively. Under harsh etching conditions that may not be the case. This possibility is not discussed herein, but a good indication that it may be occurring is a $z > 2$.[51,52]

Figure 8 plots the BE of the Ti-O component in the Ti 2p spectra vs. the Ti oxidation states in Ti metal (Ti^0), and various Ti oxides starting, with TiO (Ti^{+2}), Ti_2O_3 (Ti^{+3}) and TiO_2 (Ti^{+4}).[32] From this plot, it is reasonable to conclude that the BE differences, ΔBE, between Ti oxidation states are more or less constant and equal to ≈ 1.6 eV.[32] This example was chosen because Ti oxides can be made with a range of stoichiometries with varying oxidation states of Ti atoms and the Ti atoms are always bonded to -O atoms. Therefore, if the type of ligands attached to Ti atoms is kept the same - as in the case here - then ΔBE of Ti $2p_{3/2}$ peaks of the compound should be more or less equal with increasing Ti oxidation states. According to Fits I and IV, the ΔBE between the C-Ti^{+1}-T_z and C-Ti^{+2}-T_z components is 0.8 eV and ΔBE between the C-Ti^{+2}-T_z and C-Ti^{+3}-T_z peaks is 1.4 eV for Fit-I, and 2 eV for Fit-IV.[14,30] But based on the results shown in Figure 8, the 3 components should be more or less equally spaced in BE.

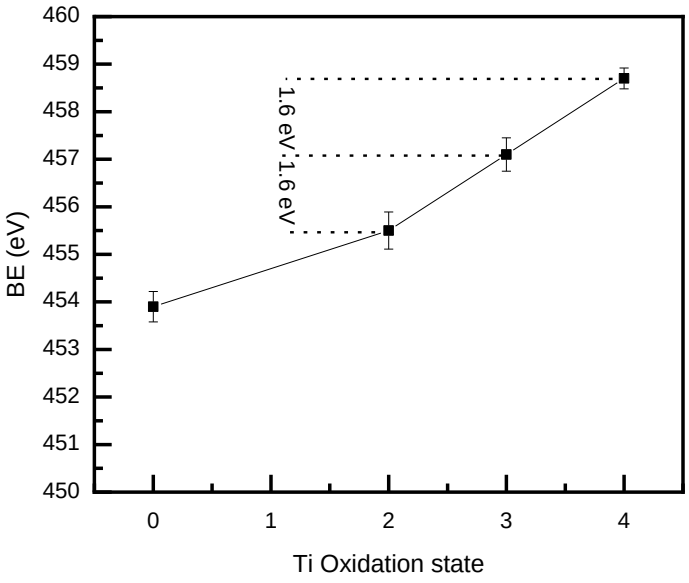

Figure 8: BE of Ti 2p peak of titanium oxide vs oxidation state of Ti in that oxide. Ti with oxidation state 0 is Ti metal.[32]

Furthermore, based on the XANES analysis by Lukatskaya *et al*.[22] it was found that the average oxidation state of Ti in $Ti_3C_2T_z$ is ~ +2.4. Based on the fractions obtained in Fit-I (Table 1) if we just consider the first 3 components - C-Ti^{+1}-O/OH, C-Ti^{+2}-O/OH, C-Ti^{+3}-O/OH - and redistribute the ratios amongst them we get new fractions which are roughly 0.31, 0.33, and 0.35, respectively. The average charge per Ti atom would thus be:

$$0.31 \times 1 + 0.33 \times 2 + 0.35 \times 3 = 2.02 \qquad (1)$$

This deviation of 0.4 in the Ti oxidation states between Fit-I and the XANES measurements, implies that the fraction of the areas under the first two peaks in Fit-I is overestimated. More importantly, it is highly unlikely that there are Ti oxidation states below +2 in MXene since Ti^{+1} states are unstable.

Regardless of the exact termination chemistries, the molecular weight of $Ti_3C_2T_z$ can be assumed to be ~200 g/mol. In a recent in-depth characterization of $Ti_3C_2T_z$ and Ti_3CNT_z MXenes by Sun *et al*.[53] they concluded - from electron paramagnetic resonance, EPR - that the Ti^{+3} concentration to be 7.08×10^{18} atoms/g of $Ti_3C_2T_z$. This translates to < 1 % Ti^{+3} atoms in $Ti_3C_2T_z$. If that is the case, it follows that both Fits-I and IV significantly overestimate the Ti^{+3} peak areas.

Therefore, at this juncture, the assumptions made in Fit-II appear to be the best way to fit the Ti 2p XPS spectra in $Ti_3C_2T_z$. In other words, we assign energies to the Ti atoms centered on the following octahedra: C-Ti-O\O\O, C-Ti-F\O\O, C-Ti-F\F\O, and C-Ti-F\F\F, respectively, depicted, schematically in Figures 9b-e. Note that as just discussed the first two are

indistinguishable.. We note in passing that this suggests that the average oxidation state of the C and O atoms are similar at ≈ -2.

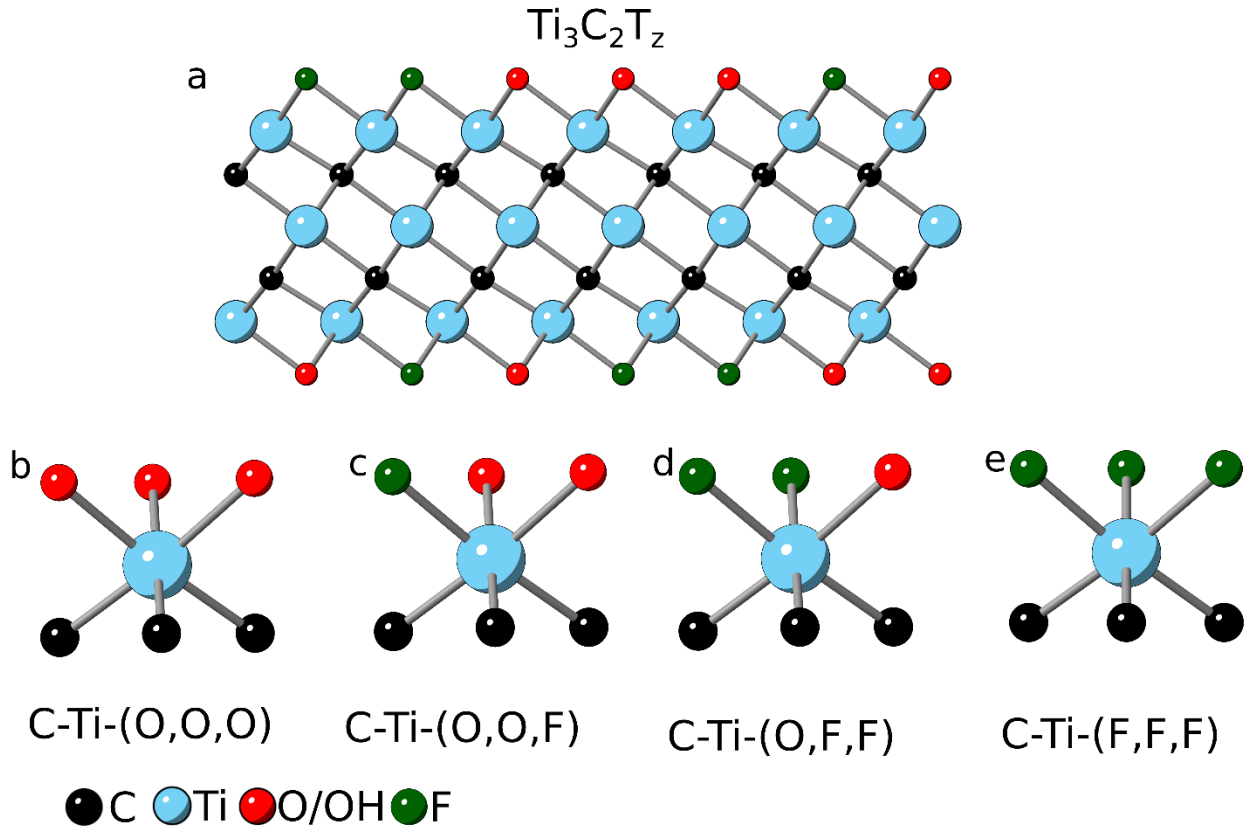

Figure 9: a) Crystal structure of $Ti_3C_2T_z$ MXene; surface Ti atoms terminated by, b) 3 O atoms c) 1 F and 2 O atoms d) 2 F and 1 O atom and, e) 3 F atoms.

Separations between the C-Ti-O/OH, C-Ti-F peaks and other component peaks:

Figure 10 plots the BEs in the Ti 2p spectra of various TiX compounds – where Ti is in a +3 or +4 oxidation state - versus a normalized EN of X, where X = S, O, F and Cl. The EN is normalized by multiplying the EN of X atoms by the X/Ti ratio to take the effect of chemistry out of the comparison. The trend is clear; increasing EN of X increases the Ti BEs more or less linearly. Similarly, the slopes are more or less independent of the Ti oxidation states that are +4

for the gray points and +3 for the red ones. [32,33] Another important observation is that for a given Ti oxidation state, ΔBE between the Ti-F and Ti-O surroundings is constant and around ~ 2.8-2.9 eV. This is important because it strongly suggests that ΔBE between the C-Ti-O\O\O and C-Ti-F\F\F sites should also be ~2.9 eV. Based on these arguments, if we assign the first Ti 2p peak at 455.0 eV to C-Ti-O\O\O, as done in Fit-II, then the C-Ti-F\F\F peaks should be around 2.9 eV higher at ≈ 458 eV. The C-Ti-O\O\F and C-Ti-O\F\F, on the other hand, should be ≈ 1 eV apart at 456 eV and 457 eV, respectively.

To confirm that interpolations from Figure 10 are meaningful, the Ti 2p BE value of $TiOF_2$[54,55] is calculated from the grey curve and found to be 459.6 eV, which matches quite well with the experimental BE of 459.5 eV (blue star in Fig. 10), found in the literature. [54,55] A similar exercise for TiOCl gives a value, based on Figure 10, of 457.8 eV, which again is in good agreement with the value of 457.9 eV reported in the literature[56] (green star Fig. 10). The arguments strongly support the placement of C-Ti-F\F\F peak 2.9 eV *higher* than its O counterpart.

Finally, it should be noted that -OH terminations are also found on MXene surfaces (see below). Here we assume they are indistinguishable from their O counterparts in the Ti 2p spectra.[57,58] Henceforth, this fitting protocol will be referred to as Fit-V.

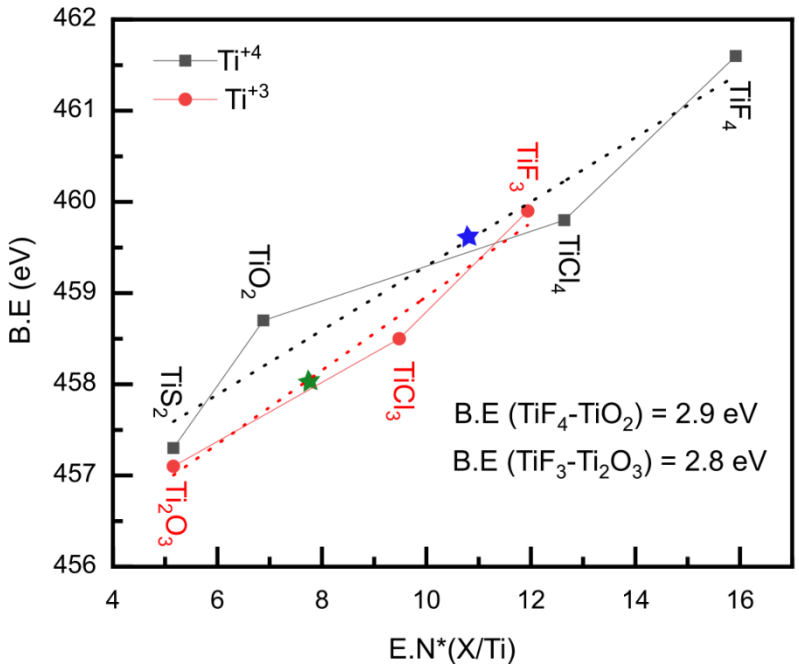

Figure 10: BE of Ti-X (X= S, O, F, Cl) component in the Ti 2p spectra vs normalized electronegativity of X atom. Gray points join Ti^{+4} compounds; red one, Ti^{+3} ones.[32,33] Blue star marks BE of $TiOF_2$ while green marks that of TiOCl.[54–56] Red and black dashed lines represent least squares fits of xxx and yy respectively. OK? If so give the equations somewhere in text.

Fit-V

In addition to the arguments made above, the following constraints were applied in our fit:

1) Similar to Fit-II, the ΔTi_{2p} for all MXene peaks was kept constant at 6.1 eV.

2) Based on XPS studies of titania, for the oxide peaks, Δ_{Ti2p} was set to 5.6 eV.[57]

3) The peak shape used for the MXene components is asymmetric and similar to that of Biesinger *et al*. as described in their XPS fittings of Ti metal.[1] [32] Symmetric Gaussian peaks, on the other hand, were used to fit the oxide contributions.

4) As discussed in the preceding section, a Tougaard background was assumed for fitting all core level spectra.

5) The FWHM of all C-Ti-Tz peaks fit under Ti $2p_{3/2}$ peak were constrained to be equal. Similarly all C-Ti-T_z peaks fit under the Ti$2p_{1/2}$ peak were constrained to be equal.

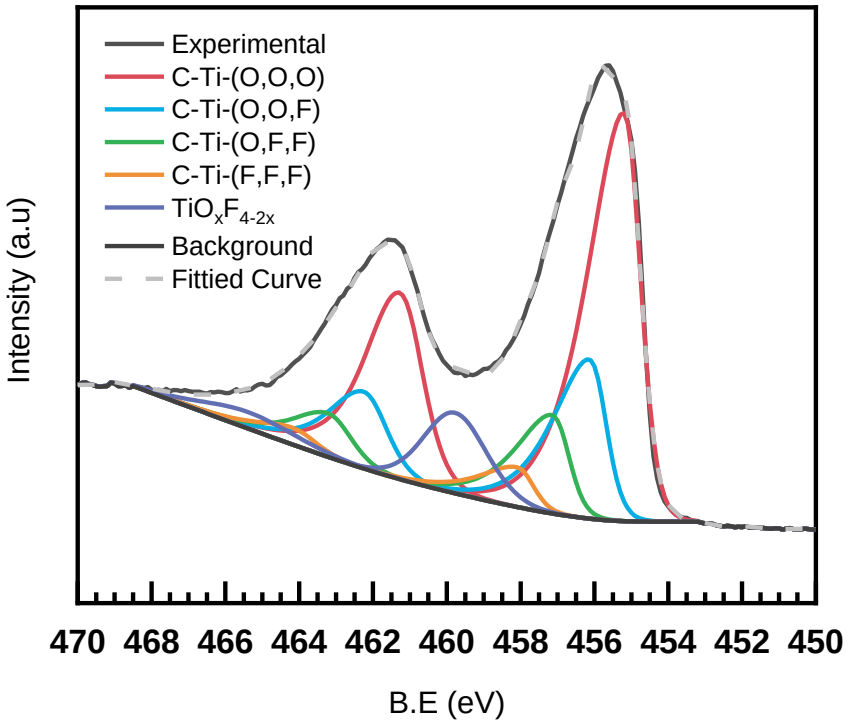

[1] In private communication Biesinger confirmed that asymmetric lines can also used for fitting Ti-C component in cubic TiC. The sample fit of cubic TiC according to Ref [32] can be found on his website - http://www.xpsfitting.com/2008/10/titanium-carbide.html.

Figure 11: XPS spectra of Ti 2p region fit according to Fit-V. Raw data used obtained from Ref [30] as was recorded from $Ti_3C_2T_z$ MXene etched from Ti_3AlC_2 MAX in 10 % HF.

Table 7: Summary of XPS peak fittings of Ti 2p spectra obtained from Ref [30] of $Ti_3C_2T_z$ synthesized by etching Ti_3AlC_2 MAX in 10% HF solution. The components were fit according to Fit-V as shown in Figure 11. Binding energies BE and FWHM values of the Ti $2p_{3/2}$ peaks are listed in columns 2 and 3, respectively. Respective numbers for Ti $2p_{1/2}$ peaks are shown in brackets.

Region	BE (eV)	FWHM (eV)	Fraction	Assigned to
Ti $2p_{3/2}$ ($2p_{1/2}$)	455.1 (461.1)	1.1 (1.5)	0.53	C-Ti-(O\O\O)
	456.0 (462.1)	1.1 (1.5)	0.22	C-Ti-(O\O\F)
	457.0 (463.1)	1.1 (1.5)	0.11	C-Ti-(O\F\F)
	457.9 (464.0)	1.1 (1.5)	0.04	C-Ti-(F\F\F)
	459.6 (465.2)	2.0 (3.0)	0.10	$TiO_{2-x}F_{2x}$

Oxides in $Ti_3C_2T_z$ MXene:

It is commonly assumed that when Ti-containing MXenes oxidize, they form TiO_2. A careful perusal of these oxidation studies,[30,49] show that clear oxide peaks emerge at BEs between 459.0 and 459.5 eV. These values are higher than the ~458.6 eV, values reported in pure TiO_2 oxides.[32] Based on the arguments made in Figure 10, it is reasonable to assume that the titania formed is not pure, but is rather doped with some F atoms and therefore those peaks should be labeled as $TiO_{2-x}F_{2x}$ instead of TiO_2. Though it is difficult to find the exact value of x, a rough estimate can be calculated by interpolating the BE values from the gray curve shown in Figure 10.

Based on all the above points, we refit the Ti 2p data by Benchakar *et al.* for $Ti_3C_2T_z$, etched in 10% HF according to Fit-V and the peak fits are shown in Figure 11. The corresponding BE values for each component are listed in Table 7.[30]

MXene synthesized in Molten Salts

Recently, Li *et al*. synthesized completely -Cl terminated MXene using a molten salt synthesis approach.[15] In their XPS fits, they used symmetric instead of asymmetric peaks, which resulted in an extra set of peaks. As discussed above, the extra peak is probably an artifact of using symmetric peaks. Further, they calibrated their spectra using the adventitious C peak which might not lead to accurate results. We refit their raw data, using the assumptions made for Fit-V as shown in Figure 12a, b, and Table 8. Recently, Lu et al. found that MXene surfaces synthesized in molten $ZnCl_2$ salts are completely saturated by Cl terminations.[59] Based on these observations there should be only 1 set of peaks corresponding to C-Ti-Cl/Cl/Cl. Unfortunately, as the Fermi edge was not scanned, we had to calibrate the spectra by setting the Ti-C-Ti peak to 282.0 eV. Doing so resulted in a C-Ti-Cl\Cl\Cl BE of 454.8 eV, which is unlikely since that is equal to the BE in the parent MAX.[60] Intriguingly, and for reasons that are unclear at this time, when we etched Ti_3AlC_2 in a non-aqueous solution, where the terminations were quite F-rich the Ti-C-Ti peak was found at 282.0 eV.[6]

Similarly, we re-fit the XPS results of Kamysbayev *et al*.[16] (Fig. 12 c-h), based on the assumption that the MXene surface is saturated with only 1 type of termination. It should be noted here that Li *et al*.[15] used C-C bond energy of 284.6 eV for calibration, while Kamysbayev *et al*. used a BE of 284.8 eV for calibration. This is a good example, of why using C-C bond BE for calibration is not recommended.

Referring back to Figures 12c-h. Here again, because the Fermi edge was not scanned, we set the Ti-C-Ti peak to 282.0 eV for calibration purposes. In the case of $Ti_3C_2Br_2$ (Fig. 12c, d) the BE of the C-Ti-Br\Br\Br bond was found to be 454.8 eV which is coincidentally equal to that C-Ti-Cl\Cl\Cl bond of $Ti_3C_2Cl_2$. Attaching highly electronegative Cl or Br terminations should shift

the BE to higher, rather than lower values. What both sets of results suggest is that the Ti-C-Ti peak in MXenes synthesized in molten salts can no longer be assumed to be at 282.0 eV.

In the case of $Ti_3C_2Te_z$ (Fig. 12e,f) the C-Ti-Te/Te/Te BE was found to be 455.0 eV which is comparable to the C-Ti-O\O\O peak of $Ti_3C_2T_z$ synthesized in F-containing acids. Even though Te is less electronegative than O, the BE of the first peak does not shift below 455.0 eV. Here again this conclusion probably stems from the Ti-C-Ti peak not being at 282.0 eV. The C-Ti-() peak – where () represents an unterminated Ti bond - (Fig. 12g,h) in the unterminated MXene samples was at 454.9 eV (Table 8) which is slightly lower than the first peak of C-Ti-O\O\O at 455.0 eV found in regular MXene. This shift of BE to lower energy is expected as electron-withdrawing surface terminations are removed from the surface. In the case of $Ti_3C_2()$, a second MXene peak at 456.7 eV (Table 8) was added to achieve a good fit. What this peak physically corresponds to is currently unclear.

These comments notwithstanding, more work needs to be carried out to examine and better understand these chemical shifts. Having a well calibrated energy scale is crucial and highly recommended.

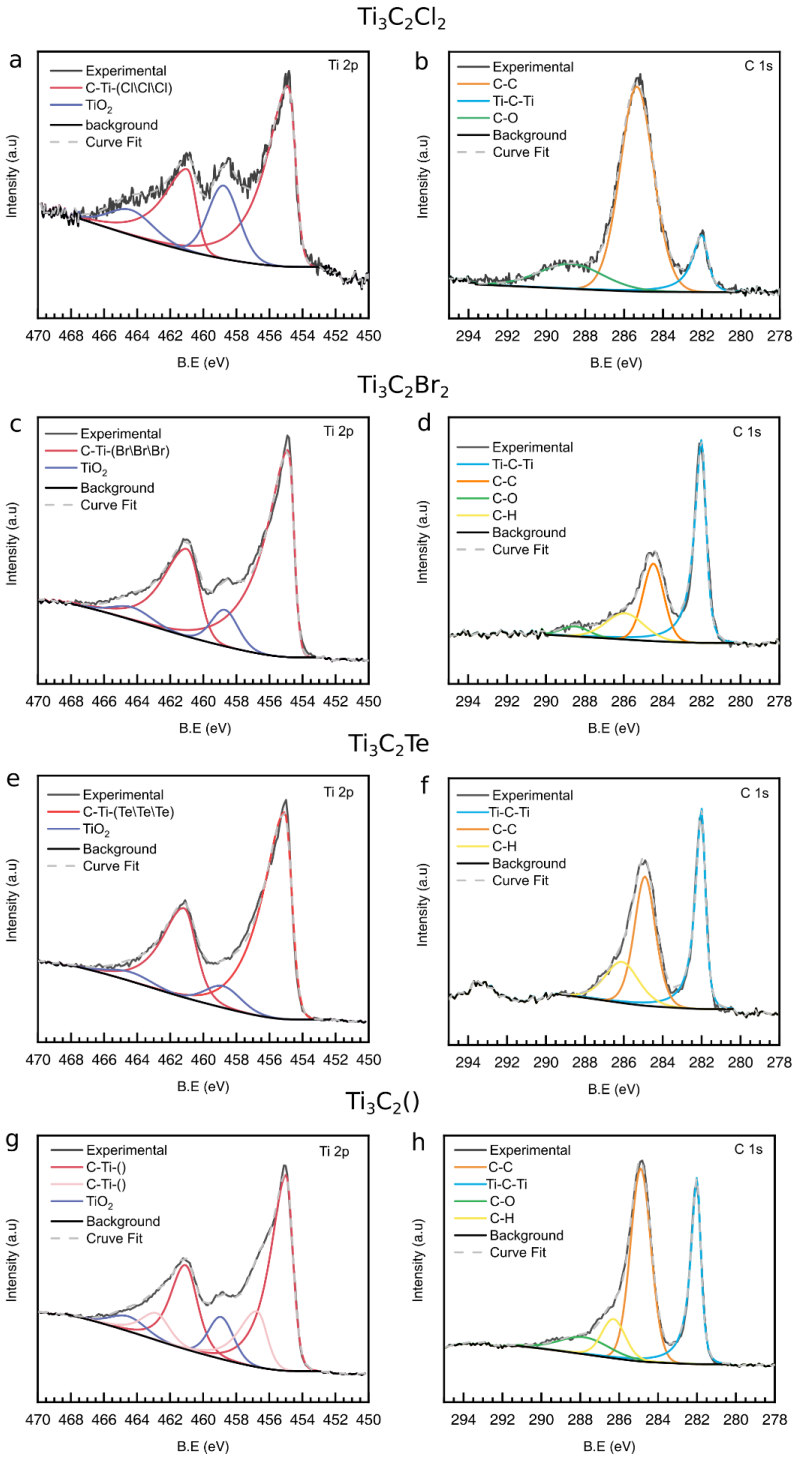

Figure 12: XPS spectra of Ti 2p and C 1s region fit according to Fit-V. Raw data obtained from Ref. [16,61] as was recorded from $Ti_3C_2T_z$ powders etched in molten salt baths starting with Ti_3AlC_2 at 550°C in case of $Ti_3C_2Cl_2$ and 650 °C in for the remaining compositions. a,b) Ti 2p and C 1s spectra of $Ti_3C_2Cl_2$; c,d) Ti 2p and C 1s spectra of $Ti_3C_2Br_2$; e,f) Ti 2p and C 1s spectra of Ti_3C_2Te ; g,h) Ti 2p and C 1s spectra of $Ti_3C_2()$,where () refers to non-terminated surfaces.

Table 8: Summary of XPS peak fittings of Ti 2p spectra obtained from Ref [16,61] of as-synthesized $Ti_3C_2T_z$ obtained by etching Ti_3AlC_2 in molten salt baths. The components were fit according to Fit-V as shown in Figure 12. Binding energies BE and FWHM values of the Ti $2p_{3/2}$ peaks are listed in columns 2 and 3, respectively. Respective numbers for Ti $2p_{1/2}$ peaks are shown in brackets.

Sample	Region	BE (eV)	FWHM (eV)	Fraction	Assigned to
$Ti_3C_2Cl_2$	Ti $2p_{3/2}$ ($2p_{1/2}$)	454.8 (460.9) 458.7 (464.3)	1.1 (1.3) 2.2 (3.2)	0.73 0.27	C-Ti-Cl\Cl\Cl TiO_2
	C 1s	282.0 285.3 288.9	0.8 2.0 2.5	0.12 0.77 0.11	Ti-C-Ti C-C C-O
$Ti_3C_2Br_2$	Ti $2p_{3/2}$ ($2p_{1/2}$)	454.8 (460.9) 458.7 (464.3)	0.9 (1.7) 1.9 (2.7)	0.88 0.12	C-Ti-Br\Br\Br TiO_2
	C 1s	282.0 284.5 285.9 288.5	0.6 1.3 2.3 1.7	0.52 0.27 0.16 0.05	Ti-C-Ti C-C C-H C-O
Ti_3C_2Te	Ti $2p_{3/2}$ ($2p_{1/2}$)	455.0 (461.1) 458.8 (464.4)	1.0 (1.7) 2.5 (3.0)	0.90 0.10	C-Ti-Te TiO_2
	C 1s	282.0 285.0 286.0	0.5 1.3 2.0	0.40 0.40 0.20	Ti-C-Ti C-C C-H
$Ti_3C_2()$	Ti $2p_{3/2}$ ($2p_{1/2}$)	454.9 (461.0) 456.7 (462.8) 458.9 (464.5)	1.0 (1.7) 1.4 (1.8) 1.7 (2.5)	0.65 0.23 0.12	C-Ti-() C-Ti-() TiO_2
	C 1s	282.0 284.9 286.3 287.8	0.5 1.2 1.4 3.0	0.30 0.47 0.12 0.11	Ti-C-Ti C-C C-H C-O

O 1s Spectra:

The O 1s spectra of Fits I-IV are all different. Fit-I has 5 component peaks: the lowest energy peak at 529.9 eV is ascribed to TiO_2; the next two peaks at 531.2 eV and 532.0 eV are assigned to C-Ti-O and C-Ti-OH, respectively. The peaks at 523.8 and 533.8 eV are allocated to alumina and adsorbed water respectively.

Persson *et al*. (Fit-II) claim that -OH terminations are not present on the MXene surfaces and the peak ascribed to C-Ti-OH in Fit-I is actually that of -O terminations that occupy bridging sites

(see Fig. 2, Fig. 3e). They argued that if the peak at 532.0 eV was due to OH, then the observed intensity loss of this peak - with increasing temperature - should reduce the total area under the O 1s curve during annealing, which is not observed. From there they conclude that the changes in peak intensities observed are due to a rearrangement of surface O atoms from bridging sites to A sites (Fig. 2).

However, Seredych *et al*. in their thermogravimetric analysis, coupled with gas mass spectroscopy (TGA-MS) studies of various MXene under flowing helium (He) gas showed that upon heating the F-atoms desorb from the MXene surface in the form of HF and not F_2 molecules.[62] If that is the case, then the -OH terminations can converted to -O, by the loss of H to HF formation. In such a scheme, the total O content would remain unchanged as observed. Though this is just a hypothesis to possibly explain the lack of O 1s area change by Persson et al., more work needs to be done to better understand this phenomenon.

Moreover, recent NMR and neutron scattering studies have proven the presence of -OH terminations.[23,53,63] Another important point to note is that vacuum annealing experiments by Persson *et al*. were carried out in ultra-high vacuum that, in principle, allow for O re-arrangements. But to understand the true nature of the O/OH terminations the samples need to re-exposed to air and water to saturate the lattice sites left unterminated after -F desorption and the sample should be rescanned.

Fit-III is similar to Fit-II, but instead of 2 possible crystallographic sites proposed in Fit-II (Fig. 2d), 3 different possible sites are proposed (Fig. 3a,h). Fit-IV uses a mix of Fits-I and II and ascribed the peaks at 529.7 and 531.2 eV to bridging and A-site O, while the peak at 532.0 eV was assigned to the C-Ti-OH bond.

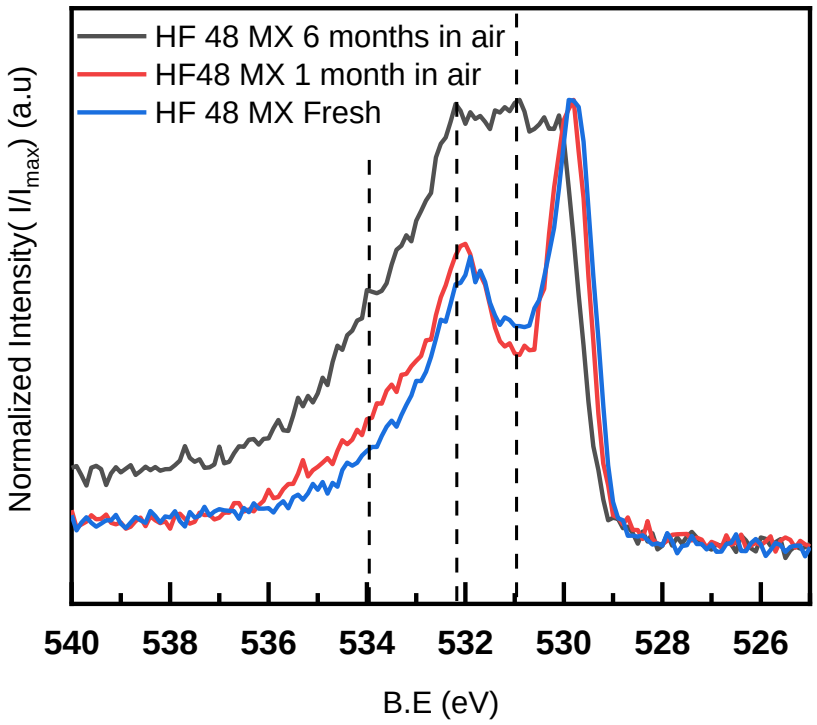

Figure 13: O 1s spectra of fresh $Ti_3C_2T_z$ MXene right after synthesis (blue) and after aging the same sample for 1 (red) and 6 months (grey).[30]

Fit-I assigns the peak at 529.9 eV to $TiO_2/TiO_{2-x}F_{2x}$, while in Fit-IV that peak is fit at 530.6 eV. They cannot both be correct. To determine which of these is correct, the data by Benchakar *et al.*[30] was replotted and the O 1s spectra of freshly synthesized MXene obtained after etching Ti_3AlC_2 in 48 % HF and its subsequent aging in the ambient atmosphere for 1 and 6 months were overlaid in Figure 13. From these results it is obvious that after 6 months a clear peak appears ~ 530.8 eV, implying that the oxide peak assignment in Fit-IV is correct. Moreover, in their study, Benchakar *et al.*[30] confirmed that peak intensity increases with the fraction of $TiO_{2-x}F_x$ in the Ti 2p region as shown by the preparation of partially oxidized $Ti_3C_2T_z$ using a FeF_3/HCl etching agent (Fig. 4). This attribution was adopted in our Fit-V.

Based on these observations it is clear that fitting O 1s spectra in $Ti_3C_2T_z$ is not trivial due to multiple overlapping contributions from surface terminations, oxides, and hydroxides. Moreover, the impurities from adventitious carbon and other organics contribute to the O 1s spectra as well and their contribution cannot be determined at this point. Therefore, more work is required to better understand the O 1s spectra.

F 1s spectra:

Fits I, III, IV all assign only one peak to F-terminations with a BE ~ 685.0 eV. Fit-II fits 2 peaks corresponding to C-Ti-F and C-Ti-(O, F) at 684.5 and 685.4 eV respectively. Depending on the etching and processing conditions impurities like AlF_3, $TiO_{2-x}F_{2x,}$ etc. are also fit under F 1s spectra. However, since F is the most EN element, the chemical shifts in its XPS spectra are small rendering the quantification of impurities difficult. Furthermore, the choice of asymmetry of the C-Ti-F peaks will also influence the quantification of any impurity peaks.

Quantification:

As discussed above, it is not trivial to quantify the surface terminations of $Ti_3C_2T_z$ flakes using XPS. What renders the problem even more intractable is that the results obtained from different characterization techniques, on nominally comparable samples, are not close. This is best seen by a perusal of the chemistries listed in Table 9, on samples obtained by etching Ti_3AlC_2 powders in 48 % HF at RT. The results of XPS analyses[14,30] are compared with those obtained by NMR[23] and neutron pair distribution function, PDF, analysis.[64] The final chemistries (column 2 in Table 9) are quite different. From Table 9 it is also clear that not only are there discrepancies in the chemistries between the various XPS studies, but also between the various techniques. Referring

to column 3 in Table 9, the O:OH ratios vary anywhere from 0.07 to 8, and the O:F varies from 0.3 to 11. Ideally, all techniques should yield comparable chemistries. The fact that they do not imply that much more work is needed in this domain. These large deviations imply that either some of these techniques cannot be used to quantify the termination chemistries or more in-depth studies are required to shed light on these discrepancies.

Table 9: Chemistries of $Ti_3C_2T_z$ samples all obtained by etching Ti_3AlC_2 in 48% HF. Charge total is calculated by assuming charge on O = - 2 and on OH and F = -1. Chemistries reported by XPS herein are ones reported in the original work.

Method	Formula	O:OH:F	T_z		Ref
			Total z	Charge total	
XPS*	$Ti_3C_2O_{0.3}(OH)_{0.02}(OH/H_2O_{ads})_{0.3}F_{1.2}$	1:0.07:4	1.52 (1.82)	1.82 (2.12)	[14]
XPS^	$Ti_3C_{2.03}O(i)_{0.43}O(ii)_{0.06}(OH)_{0.3}F_{1.34}$	1:0.6:2.7	2.13	2.62	[30]
NMR‡	$Ti_3C_2O_{0.84}(OH)_{0.06}F_{0.25}$	1:0.07:0.3	1.15	2.0	[23]
PDF‖	$Ti_3C_2O_{0.1}(OH)_{0.8}F_{1.1}$	1:8:11	2.0	2.1	[65]

*In Ref [14] Halim *et al*. calculated values in parenthesis assuming all the H_2O as OH, the values outside the parenthesis are assuming otherwise.
^ In Ref [30] Benchakar *et al*. fit 2 sites for O terminations denoted (i) and (ii) for calculation of T_z both have been added.
‡ In Ref [23] Hope *et al*. assumed a charge total of T_z equal to + 2 and back-calculated the stoichiometry.
‖ In Ref [64] Wang *et al*. assumed z = 2 and back-calculated the stoichiometry.

In Figure 14, we refit the results of Benchakar *et al*.[30] for Ti_3AlC_2 etched in 10 % HF using Fit-V. The results are summarized in Table 10. The C 1s spectra were fit with 1 asymmetric peak at 282.0 eV corresponding to C atoms centered in Ti-octahedra. The other C 1s peaks were ascribed to adventitious carbon.

In the O 1s spectra, the first peak at 529.8 eV was ascribed to C-Ti-O\O\O. The peak at ~532.0 eV is ascribed to the C-Ti-OH bond in Fits-I and IV and to a C-Ti-O/F bond by Fit-II, where O/F corresponds to the O co-adsorbed with F atoms. Moreover, by coupling XPS and Raman spectroscopy and by comparing $Ti_3C_2T_z$ etched with HF10% and HF48%, which in turn allowed

for the variation of the OH/O ratio, Benchakar *et al.* [27] show that this peak can, with a large degree of certainty, be attributed to C-Ti-OH. Nevertheless, a contribution of the C-Ti-O/F bond in this peak cannot be excluded. Therefore, in Fit-V we assume that the 532.0 eV peak is probably a convolution of C-Ti-OH and C-Ti-(O,F) moieties. The 530.8 eV peak was ascribed to O in $TiO_{2-x}F_{2x}$ (Fig. 13,14).[54]

The F 1s spectra were fit with only one asymmetric peak at 684.9 eV. Given that the BE of the F 1s peak in $TiO_{2-x}F_{2x}$ is also ~ 685.0 eV[54,55] it is currently not possible to deconvolute the peak.

For the quantification, shown in Table 10, a few assumptions were made:

1) The BE of the $TiO_{2-x}F_{2x}$ peak in the Ti 2p spectra was constrained between 459.0-460.0 eV. We further assume x = ½. This implies the oxide chemistry is $TiO_{1.5}F$. It should be noted that the BE of $TiOF_2$ shown in Figure 10 was obtained from prior work where the presence of $TiOF_2$ was also confirmed by XRD. In the case of oxide formation due to oxidation of $Ti_3C_2T_z$, XPS indicates a BE closer to $TiOF_2$. XRD measurements, however, indicate the presence of rutile or anatase TiO_2.[49] Prior work by Czoska *et al.* on F-doped TiO_2 found that some F atoms can play two roles: Some replace O atoms in the titania lattice and others replace surface hydroxyl groups.[66] We believe a similar phenomenon also occurs on the surface of TiO_2 formed on MXene surfaces, because XPS indicates a higher F-content compared to a bulk analysis by XRD. Therefore, we assume an approximate stoichiometry of $TiO_{1.5}F$. Further, depending on the etching condition usedMashtalir[67] and Benchakar *et al.*[8] from their XRD and Raman spectroscopy analysis, respectively, also observed the formation of $TiOF_2$ and/or $TiO_{2-x}F_{2x}$ in MXene samples. It should be noted since TiO_2 is a semiconductor its corresponding peaks might shift to higher BE due to local charging, band bending, etc. However, previous XPS studies of

TiO_2 on metallic substrates, [68][69], found that the BE of the Ti $2p_{3/2}$ peak ascribed to TiO_2 was below 459.0 eV. It is thus reasonable to assume here, given the conductive nature of $Ti_3C_2T_z$, that the TiO_2 peaks should *not* move to higher BE and that the shifts are solely due to F on the surface and/or the bulk of the oxide. But to confirm these conjectures more detailed preferably in-situ oxidation studies of $Ti_3C_2T_z$ should be carried out.

3) The BE of the titanium oxide peak in the O 1s spectra was assumed to be 530.8 eV (according to the O 1s discussion based on Figure 13). The area was constrained such that the Ti:O ratio in the oxide stoichiometry is 1:1.5 based on a $TiO_{1.5}F$ formula.

4) Since we assume that the $TiO_{2-x}F_{2x}$ peak overlaps with the C-Ti-F peak in the F1s region, the area of the oxide peak was subtracted from the total peak area. The oxide peak area subtracted was constrained such that the Ti:F ratio in oxide stoichiometry was 1:1, again based on the assumed $TiO_{1.5}F$ formula.

5) Minimal impurities were assumed. Other than adventitious carbon and titanium oxyfluoride no other impurities were taken into consideration during fitting.

Based on these fits, the chemical formulae obtained (Table 11) agree well with 2 general well-established structural constraints. The first is that the Ti:C ratio of MXene is roughly 3:2. The second is that z in $T_z \sim 2$. The latter is an excellent assumption since this is the value one obtains if one were to fill the close-packed sites on the Ti surfaces. Said otherwise it is the value one would obtain if every termination atom is bonded to the 3 Ti atoms. DFT calculations have shown that the energy of the system increases rapidly for $z > 2$.[70] Values of $z > 2.5$ suggest that termination atoms are substituting for C atoms in the Ti_3C_2 layers.[51]

Values of z < 2 would imply the presence of bare Ti bonds which is impossible given its reactivity. Even if ultrahigh vacuum, Ti surfaces are rapidly covered in a layer of oxygen, let alone ambient atmospheres. If any XPS analysis results in z <<2, that should be taken as a large red flag that the analysis is seriously flawed. These constraints are important and deviations from these values suggest either problems with the fits and/or very unusual processing/storing protocols.

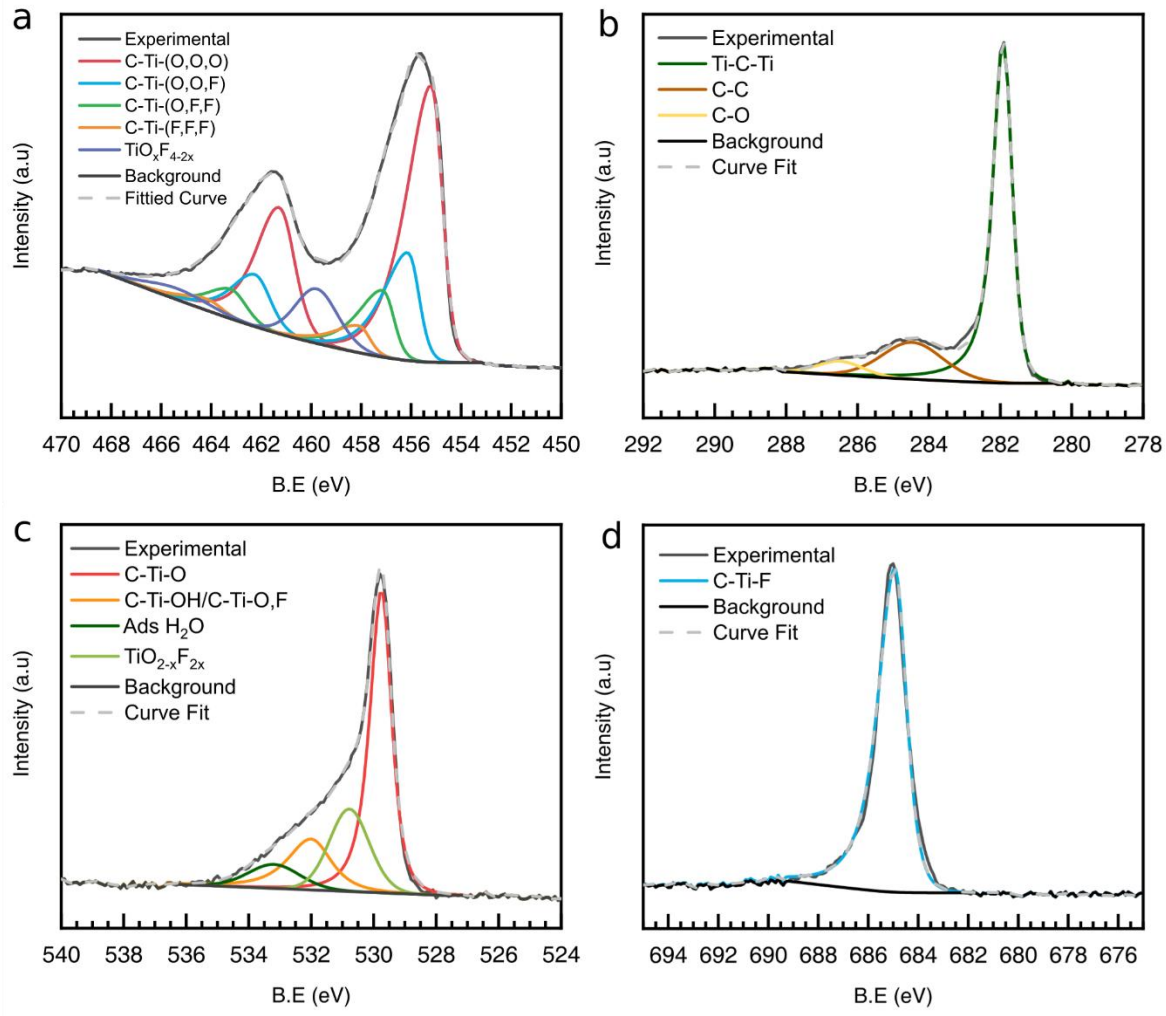

Figure 14: Fit-V of XPS spectra of $Ti_3C_2T_z$ obtained after etching Ti_3AlC_2 in 10% HF, a) Ti 2p, b) C 1s, c) O 1s and, d) F 1s regions. Raw data obtained from Ref [30].

Table 10: Summary of XPS peak fittings based on Fit-V for MXene synthesized using 10% HF as shown in Figure 14. Binding energies BE and FWHM values of the Ti $2p_{3/2}$ peaks are listed in columns 2 and 3, respectively. Respective numbers for Ti $2p_{1/2}$ peaks are shown in brackets.

Region	BE (eV)	FWHM (eV)	Fraction	Assigned to
Ti $2p_{3/2}$ ($2p_{1/2}$)	455.1 (461.1)	1.1 (1.5)	0.53	C-Ti-(O\O\O)
	456.0 (462.1)	1.1 (1.5)	0.22	C-Ti-(O\O\F)
	457.0 (463.1)	1.1 (1.5)	0.11	C-Ti-(O\F\F)
	457.9 (464.0)	1.1 (1.5)	0.04	C-Ti-(F\F\F)
	459.6 (465.2)	2.0 (3.0)	0.10	$TiO_{2-x}F_{2x}$
C 1s	282.0	0.6	0.74	Ti-C-Ti
	284.4	1.9	0.20	C-C
	286.5	1.5	0.06	C-O
O 1s	529.8	0.9	0.51	C-Ti-O
	532.0	1.0	0.18	C-Ti-OH/C-Ti-O/F
	530.8	2.0	0.23	$TiO_{2-x}F_{2x}$
	533.4	1.5	0.08	Adsorbed H_2O
F 1s	684.9	1.1	1	C-Ti-F/$TiO_{2-x}F_{2x}$

Table 11: MXene chemistries calculated after applying Fit-V to $Ti_3C_2T_z$ spectra obtained from Ti_3AlC_2 powders etched in various media and conditions indicated in column 1. All raw data obtained from Ref [30]. Bold entries are those obtained using Fit-IV on results published in Ref. 30. Total charge on terminations is calculated assuming O = -2 and OH and F= -1. O_F stands for O co-absorbed with F. As we cannot differentiate between OH and O_F in Fit-V in column 5 we assume all the 532.0 eV peaks in O 1s to be only O_F while in column 6 we assume it be all OH while calculating the charge total of T_z. Fit-IV this differentiation is not made so charge total is given in column 4.

Etchant	**Chemistry**	**z (moles)**	**Charge total of Tz**		
			Fit-IV Ref [27]	**Assuming all O_F**	**Assuming all OH**
HF- 48 %	$Ti_3C_{1.94}O_{0.39}(O_F/OH)_{0.25}F_{1.5}$	2.14	-	- 2.8	- 2.53
	$Ti_3C_{2.03}O_{0.49}(OH)_{0.30}F_{1.34}$	**2.13**	**-2.62**	-	-
HF - 10 %	$Ti_3C_{2.1}O_{0.81}(O_F/OH)_{0.20}F_{0.89}$	1.9		- 2.91	- 2.71
	$Ti_3C_{2.08}O_{1.04}(OH)_{0.19}F_{0.61}$	**1.84**	**-2.88**	-	-
LiF+HCl (60°C)	$Ti_3C_{2.1}$ $O_{0.98}(O_F/OH)_{0.15}F_{0.8}$	1.93	--	- 3.07	- 2.91
	$Ti_3C_{1.86}O_{1.0}(OH)_{0.16}F_{0.70}$	**1.86**	**-2.86**	-	-
LiF+HCl (RT)	$Ti_3C_{2.0}$ $O_{0.85}(O_F/OH)_{0.30}F_{0.94}$	2.09	-	- 3.24	- 2.94
	$Ti_3C_{1.94}O_{0.94}(OH)_{0.17}F_{0.75}$	**1.86**	**-2.80**	-	-

Therefore, Fit-V can also be used for the overall quantification of surface terminations. $Ti_3C_2T_z$ etched in 48 % HF has nearly double the F-content compared to MXene synthesized using milder etching methods (Table 11). Also, the charge calculated based on T_z was slightly lower in MXene synthesized using 48% HF compared to MXene synthesized using milder etching methods. For the latter, the average charge of T_z is between - 2.9 and - 3.3. At - 2.5 to - 2.8, it is slightly lower in samples etched in 48 % HF. Based on these results if we assume an average T_z charge of 3.3 considering all the contribution under the 532.0 eV in O 1s to be from the C-Ti-(O,F) and assuming the Ti oxidation state to be +2.4 we can calculate the oxidation state to C to be ≈ – 1.95. Doing similar calculation but instead ascribing the peak at 532.0 eV completely to C-Ti-OH and assuming an average T_z charge of 2.9, the oxidation state of C is -2.15. In other words, in both cases, the average oxidation of C is ≈ - 2. If that is the case, it is not surprising that it is difficult to differentiate in the Ti 2p spectra between, the central Ti atoms and those near surfaces terminated by O\O\O.

The average depth of analysis using XPS is generally around 5-10 nm.[28,71] Unlike bulk materials that can be assumed to be homogenous for nanomaterials like MXene which are only 1 nm thick, the XPS quantification is averaging over several MXene flakes. For example, assuming a 200 µm spot size of the X-ray beam and a probing depth of 10 nm gives us average quantification over 10^6 MXene flakes. Therefore, we are not collecting signals from just the surface terminations but also from the core of each flake, the interlayer intercalated species like cations and water molecules, and from impurities like oxides, etching residues, etc. Also, the subsurface photoelectrons will have higher scattering lengths compared to the ones on the surface, due to which subsurface MXenes flakes will tend to show slightly different chemistry than the MXene flakes on the surface of the sample due to this artifact. Therefore because of

these problems, it is difficult to obtain exact chemistries of bulk MXene samples, but rough estimations can be obtained via our proposed fittings.

Conclusions

In this work, we compare and contrast four methods in the literature used to fit the XPS spectra of $Ti_3C_2T_z$. Confusingly, these models make quite different assumptions and each results in different termination chemistry. According to our analysis, none of the existing methods is perfect.

We also make the case that the most physically tenable approach is to fit the Ti $2p_{3/2}$ spectra based on the apexes of the octahedra that surround the Ti atoms. Consequently, we assign the peak at 455.0 eV to C-Ti-C and/or C-Ti-O\O\O octahedra. It is difficult to distinguish between the two. The peaks at 456.0, 457.0, 457.9 eV, are assigned to the C-Ti-O\O\F, C-Ti-O\F\F, C-Ti-F\F\F, octahedra, respectively. The peak at 459.2 eV is assigned to $TiO_{2-x}F_{2x}$. The BE of the C atoms sitting in the Ti-octahedra in the MX layers is almost always at 282.0 eV. This value appears to be independent of almost all variables except, possibly, when the Ti_3AlC_2 is etched in molten salts.

The $Ti_3C_2T_z$ affiliated F 1s spectra, like C 1s, were fit with only 1 peak corresponding to F-terminations. Quantifying non-MXene F contributions is much more difficult compared to C 1s and should be avoided if at all possible.

Fitting of the O 1s spectra was the most ambiguous and a lot more work needs to be carried out to understand the various O terminations. However, we assign the peak at 529.8 eV to C-Ti-O

and that at 532.0 eV to C-Ti-OH and/or C-Ti-O/F. Apart from these two, MXene peaks at 530.8 and 533.4 eV were ascribed to $TiO_{2-x}F_{2x}$ and adsorbed H_2O, respectively.

Asymmetric line shapes, similar to those used for fitting spectra of Ti metal, are used in our proposed model. But given that the behavior of scattered electrons is different in MXenes compared to pure Ti metal these peak shapes need to be further optimized specifically for MXenes. This is non-trivial as we need to consider interflake and intraflake transport of electrons between MXene sheets and also the role of interlayer species, impurities, etc. Improved synthesis of MXenes flakes coupled with a better understanding of electronic transport in MXenes can help us model better peak shapes specifically for $Ti_3C_2T_z$ MXenes.

Hopefully, future studies can lead to a better understanding leading to more accurate quantification. The help of modelization by DFT calculations is probably required. Finally, this review was focused mainly on the $Ti_3C_2T_z$ which is by far the most studied MXene and even here the XPS fits are not completely understood therefore utmost care should be taken while fitting other MXene compositions as findings from $Ti_3C_2T_z$ may or may not directly translate to those fittings.

Fitting Methods:

CasaXPS Version 2.3.19PR1.0 software was used for peak fitting. The XPS spectra were calibrated by setting the valence edge to zero, which was calculated by fitting the valence edge with a step-down function and setting the intersection to 0 eV. Because MXenes are electrically conductive, all MXene related peaks were fit using an asymmetric Lorentzian line shape. The oxide peaks, on the other hand,

were fit using a symmetric Gaussian/Lorentzian line shape. The background was determined using the Tougaard algorithm, which is a built-in function in the CasaXPS software.

To calculate the elemental ratios the global elemental ratios were first calculated by considering the total areas under the curves and the relative sensitivity factors for each element. This was done with the help of internal tools provided by CasaXPS software. Further, global elemental ratios obtained were multiplied by the percentage of photoemission spectra contribution by the MXene or oxide component. This was calculated for each element individually to obtain the chemical formula shown in Table 11.

Acknowledgment:

This work was funded by the Division of Materials Research of NSF (DMR 1740795). IC2MP acknowledges financial support from the “Agence National de la Recherche” (reference ANR-18-CE08-014 – MXENECAT project), the European Union (ERDF), the "Région Nouvelle Aquitaine" and the French research ministry (Ph.D. thesis of M. Benchakar).

We would like to acknowledge and thank Drs. Joseph Halim, Dr. Qing Huang, Dr. Dmitri Talapin, Dr. Johanna Rosen and Dr. Per Persson for sharing their raw data used herein. We would also like to acknowledge Drs. Farley, Biesinger and Tougaard for their advice on peak fitting and background subtraction.

References:

[1] M. Naguib, M. Kurtoglu, V. Presser, J. Lu, J. Niu, M. Heon, L. Hultman, Y. Gogotsi, M. W. Barsoum, *Adv. Mater*. **2011**, *23*, 4248.

[2] B. Anasori, M. R. Lukatskaya, Y. Gogotsi, *Nat. Rev. Mater.* **2017**, *2*, 16098.

[3] L. Verger, C. Xu, V. Natu, H.-M. Cheng, W. Ren, M. W. Barsoum, *Curr. Opin. Solid State Mater. Sci.* **2019**, DOI 10.1016/j.cossms.2019.02.001.

[4] V. Natu, M. Clites, E. Pomerantseva, M. W. Barsoum, *Mater. Res. Lett.* **2018**, *6*, 230.

[5] S. Intikhab, V. Natu, J. Li, Y. Li, Q. Tao, J. Rosen, M. W. Barsoum, J. Snyder, *J. Catal.* **2019**, *371*, 325.

[6] V. Natu, R. Pai, M. Sokol, M. Carey, V. Kalra, M. W. Barsoum, *Chem* **2020**, *6*, 616.

[7] K. Montazeri, M. Currie, L. Verger, P. Dianat, M. W. Barsoum, B. Nabet, *Adv. Mater.* **2019**, *31*, 1903271.

[8] M. Benchakar, V. Natu, T. A. Elmelegy, M. Sokol, J. Snyder, C. Comminges, C. Morais, S. Célérier, A. Habrioux, M. W. Barsoum, *J. Electrochem. Soc.* **2020**.

[9] M. Carey, Z. Hinton, V. Natu, R. Pai, M. Sokol, N. J. Alvarez, V. Kalra, M. W. Barsoum, *Cell Reports Phys. Sci.* **2020**, *1*, 100042.

[10] F. Shahzad, M. Alhabeb, C. B. Hatter, B. Anasori, S. Man Hong, C. M. Koo, Y. Gogotsi, *Science (80-.).* **2016**, *353*, 1137.

[11] M. Sokol, V. Natu, S. Kota, M. W. Barsoum, *Trends Chem.* **2019**, DOI 10.1016/j.trechm.2019.02.016.

[12] Z. M. Sun, *Int. Mater. Rev.* **2011**, *56*, 143.

[13] M. W. Barsoum, *MAX Phases*, Wiley-VCH Verlag GmbH & Co. KGaA, Weinheim, Germany, **2013**.

[14] J. Halim, K. M. Cook, M. Naguib, P. Eklund, Y. Gogotsi, J. Rosen, M. W. Barsoum, *Appl. Surf. Sci.* **2016**, *362*, 406.

[15] M. Li, J. Lu, K. Luo, Y. Li, K. Chang, K. Chen, J. Zhou, J. Rosen, L. Hultman, P. Eklund, P. O. Å. Persson, S. Du, Z. Chai, Z. Huang, Q. Huang, *J. Am. Chem. Soc.* **2019**, *141*, 4730.

[16] V. Kamysbayev, A. S. Filatov, H. Hu, X. Rui, F. Lagunas, D. Wang, R. F. Klie, D. V. Talapin, *Science (80-.).* **2020**, eaba8311.

[17] M. Ghidiu, J. Halim, S. Kota, D. Bish, Y. Gogotsi, M. W. Barsoum, *Chem. Mater.* **2016**, *28*, 3507.

[18] V. Natu, M. Sokol, L. Verger, M. W. Barsoum, *J. Phys. Chem. C* **2018**, *122*, 27745.

[19] Z. Lin, H. Shao, K. Xu, P.-L. Taberna, P. Simon, *Trends Chem.* **2020**, *2*, 654.

[20] T. Schultz, N. C. Frey, K. Hantanasirisakul, S. Park, S. J. May, V. B. Shenoy, Y. Gogotsi, N. Koch, *Chem. Mater.* **2019**, acs. chemmater.9b00414.

[21] X. Jiang, A. V. Kuklin, A. Baev, Y. Ge, H. Ågren, H. Zhang, P. N. Prasad, *Phys. Rep.* **2020**, *848*, 1.

[22] M. R. Lukatskaya, S.-M. Bak, X. Yu, X.-Q. Yang, M. W. Barsoum, Y. Gogotsi, *Adv. Energy Mater.* **2015**, *5*, 1500589.

[23] M. A. Hope, A. C. Forse, K. J. Griffith, M. R. Lukatskaya, M. Ghidiu, Y. Gogotsi, C. P. Grey, *Phys. Chem. Chem. Phys.* **2016**, *18*, 5099.

[24] K. J. Harris, M. Bugnet, M. Naguib, M. W. Barsoum, G. R. Goward, *J. Phys. Chem. C*

2015, *119*, 13713.

[25] A. Sarycheva, Y. Gogotsi, *Chem. Mater.* **2020**, *32*, 3480.

[26] L. H. Karlsson, J. Birch, J. Halim, M. W. Barsoum, P. O. Å. Persson, *Nano Lett.* **2015**, *15*, 4955.

[27] D. Magne, V. Mauchamp, S. Célérier, P. Chartier, T. Cabioc'h, *Phys. Chem. Chem. Phys.* **2016**, *18*, 30946.

[28] S. Hofmann, *Auger- and X-Ray Photoelectron Spectroscopy in Materials Science*, Springer Berlin Heidelberg, Berlin, Heidelberg, **2013**.

[29] I. Persson, L.-Å. Näslund, J. Halim, M. W. Barsoum, V. Darakchieva, J. Palisaitis, J. Rosen, P. O. Å. Persson, *2D Mater.* **2017**, *5*, 015002.

[30] M. Benchakar, L. Loupias, C. Garnero, T. Bilyk, C. Morais, C. Canaff, N. Guignard, S. Morisset, H. Pazniak, S. Hurand, P. Chartier, J. Pacaud, V. Mauchamp, M. W. Barsoum, A. Habrioux, S. Célérier, *Appl. Surf. Sci.* **2020**, *530*, 147209.

[31] M. Guemmaz, A. Mosser, J.-C. Parlebas, *J. Electron Spectros. Relat. Phenomena* **2000**, *107*, 91.

[32] M. C. Biesinger, L. W. M. Lau, A. R. Gerson, R. S. C. Smart, *Appl. Surf. Sci.* **2010**, *257*, 887.

[33] C. Mousty-Desbuquoit, J. Riga, J. J. Verbist, *Inorg. Chem.* **1987**, *26*, 1212.

[34] M. Khazaei, M. Arai, T. Sasaki, C.-Y. Chung, N. S. Venkataramanan, M. Estili, Y. Sakka, Y. Kawazoe, *Adv. Funct. Mater.* **2013**, *23*, 2185.

[35] G. Greczynski, L. Hultman, *ChemPhysChem* **2017**, *18*, 1507.

[36] M. T. Anthony, M. P. Seah, *Surf. Interface Anal.* **1984**, *6*, 107.

[37] R. I. . Blyth, H. Buqa, F. . Netzer, M. . Ramsey, J. . Besenhard, P. Golob, M. Winter, *Appl. Surf. Sci.* **2000**, *167*, 99.

[38] J. Halim, M. R. Lukatskaya, K. M. Cook, J. Lu, C. R. Smith, L.-Å. Näslund, S. J. May, L. Hultman, Y. Gogotsi, P. Eklund, M. W. Barsoum, *Chem. Mater.* **2014**, *26*, 2374.

[39] J. Halim, I. Persson, P. Eklund, P. O. Å. Persson, J. Rosen, *RSC Adv.* **2018**, *8*, 36785.

[40] J. Halim, S. Kota, M. R. Lukatskaya, M. Naguib, M.-Q. Zhao, E. J. Moon, J. Pitock, J. Nanda, S. J. May, Y. Gogotsi, M. W. Barsoum, *Adv. Funct. Mater.* **2016**, *26*, 3118.

[41] R. Meshkian, H. Lind, J. Halim, A. El Ghazaly, J. Thörnberg, Q. Tao, M. Dahlqvist, J. Palisaitis, P. O. Å. Persson, J. Rosen, *ACS Appl. Nano Mater.* **2019**, *2*, 6209.

[42] J. Halim, An X-Ray Photoelectron Spectroscopy Study of Multilayered Transition Metal Carbides (MXenes), Drexel University, **2016**.

[43] R. Nyholm, N. Martensson, A. Lebugle, U. Axelsson, *J. Phys. F Met. Phys.* **1981**, *11*, 1727.

[44] M. Repoux, *Surf. Interface Anal.* **1992**, *18*, 567.

[45] J. Luthin, C. Linsmeier, *Phys. Scr.* **2001**, *T91*, 134.

[46] F. Kong, X. He, Q. Liu, X. Qi, Y. Zheng, R. Wang, Y. Bai, *Electrochim. Acta* **2018**, *265*, 140.

[47] Y. Cao, Q. Deng, Z. Liu, D. Shen, T. Wang, Q. Huang, S. Du, N. Jiang, C.-T. Lin, J. Yu, *RSC Adv.* **2017**, *7*, 20494.

[48] K. Krishnamoorthy, P. Pazhamalai, S. Sahoo, S.-J. Kim, *J. Mater. Chem. A* **2017**, *5*, 5726.

[49] V. Natu, J. L. Hart, M. Sokol, H. Chiang, M. L. Taheri, M. W. Barsoum, *Angew. Chemie Int. Ed.* **2019**, DOI 10.1002/anie.201906138.

[50] X. Wang, C. Garnero, G. Rochard, D. Magne, S. Morisset, S. Hurand, P. Chartier, J. Rousseau, T. Cabioc'h, C. Coutanceau, V. Mauchamp, S. Célérier, *J. Mater. Chem. A* **2017**, *5*, 22012.

[51] Y. Yoon, T. A. Le, A. P. Tiwari, I. Kim, M. W. Barsoum, H. Lee, *Nanoscale* **2018**, *10*, 22429.

[52] J. Halim, K. M. Cook, P. Eklund, J. Rosen, M. W. Barsoum, *Appl. Surf. Sci.* **2019**, *494*, 1138.

[53] W. Sun, H. Wang, L. Vlcek, J. Peng, A. B. Brady, N. C. Osti, E. Mamontov, M. Tyagi, J. Nanda, S. G. Greenbaum, P. R. C. Kent, M. Naguib, *Adv. Mater. Interfaces* **2020**, *7*, 1902207.

[54] S. V. Gnedenkov, D. P. Opra, S. L. Sinebryukhov, V. G. Kuryavyi, A. Y. Ustinov, V. I. Sergienko, *J. Alloys Compd.* **2015**, *621*, 364.

[55] C. Z. Wen, Q. H. Hu, Y. N. Guo, X. Q. Gong, S. Z. Qiao, H. G. Yang, *Chem. Commun.* **2011**, *47*, 6138.

[56] M. Sing, S. Glawion, M. Schlachter, M. R. Scholz, K. Goß, J. Heidler, G. Berner, R.

Claessen, *Phys. Rev. Lett.* **2011**, *106*, 056403.

[57] M. C. Biesinger, B. P. Payne, A. P. Grosvenor, L. W. M. Lau, A. R. Gerson, R. S. C. Smart, *Appl. Surf. Sci.* **2011**, *257*, 2717.

[58] E. McCafferty, J. P. Wightman, *Surf. Interface Anal.* **1998**, *26*, 549.

[59] J. Lu, I. Persson, H. Lind, J. Palisaitis, M. Li, Y. Li, K. Chen, J. Zhou, S. Du, Z. Chai, Z. Huang, L. Hultman, P. Eklund, J. Rosen, Q. Huang, P. O. Å. Persson, *Nanoscale Adv.* **2019**, *1*, 3680.

[60] S. Myhra, J. A. A. Crossley, M. W. Barsoum, *J. Phys. Chem. Solids* **2001**, *62*, 811.

[61] M. Li, J. Lu, K. Luo, Y. Li, K. Chang, K. Chen, J. Zhou, J. Rosen, L. Hultman, P. Eklund, P. O. Å. Persson, S. Du, Z. Chai, Z. Huang, Q. Huang, *J. Am. Chem. Soc.* **2019**, *141*, 4730.

[62] M. Seredych, C. E. Shuck, D. Pinto, M. Alhabeb, E. Precetti, G. Deysher, B. Anasori, N. Kurra, Y. Gogotsi, *Chem. Mater.* **2019**, *31*, 3324.

[63] T. Kobayashi, Y. Sun, K. Prenger, D. Jiang, M. Naguib, M. Pruski, *J. Phys. Chem. C* **2020**, *124*, 13649.

[64] Y. Wang, H. Dou, J. Wang, B. Ding, Y. Xu, Z. Chang, X. Hao, *J. Power Sources* **2016**, *327*, 221.

[65] H.-W. Wang, M. Naguib, K. Page, D. J. Wesolowski, Y. Gogotsi, *Chem. Mater.* **2016**, *28*, 349.

[66] A. M. Czoska, S. Livraghi, M. Chiesa, E. Giamello, S. Agnoli, G. Granozzi, E. Finazzi, C.

Di Valentin, G. Pacchioni, *J. Phys. Chem. C* **2008**, *112*, 8951.

[67] O. Mashtalir, Chemistry of Two-Dimensional Transition Metal Carbides (MXenes), Drexel University, **2015**.

[68] C. M. Greenlief, J. M. White, C. S. Ko, R. J. Gorte, *J. Phys. Chem.* **1985**, *89*, 5025.

[69] G. Lu, S. L. Bernasek, J. Schwartz, *Surf. Sci.* **2000**, *458*, 80.

[70] M. Ashton, K. Mathew, R. G. Hennig, S. B. Sinnott, *J. Phys. Chem. C* **2016**, *120*, 3550.

[71] P. J. Cumpson, *Appl. Surf. Sci.* **1999**, *144–145*, 16.